https://doi.org/10.1016/j.trd.2023.103644



# Electrification of a Citywide Bus Network: A Data-driven Micro-simulation Approach

Shiqi Wang[1], Yuze Li[1,2], Anthony Chen[3,5], Chengxiang Zhuge[1,4,5,6*]

[1] Department of Land Surveying and Geo-Informatics, The Hong Kong Polytechnic University, Hung Hom, Kowloon, Hong Kong, China

[2] Beijing Glory PKPM Technology Co., Ltd., Beijing, China

[3] Department of Civil and Environmental Engineering, The Hong Kong Polytechnic University, Hung Hom, Kowloon, Hong Kong, China

[4] Research Institute for Sustainable Urban Development, The Hong Kong Polytechnic University, Hung Hom, Kowloon, Hong Kong, China

[5] Smart Cities Research Institute, The Hong Kong Polytechnic University, Hong Kong, China

[6] The Hong Kong Polytechnic University Shenzhen Research Institute, Shenzhen, China

Email addresses: Shiqi Wang (shiqi-anya.wang@connect.polyu.hk); Yuze Li (yuzee.li@connect.polyu.hk); Anthony Chen (anthony.chen@polyu.edu.hk); Chengxiang Zhuge* (Corresponding Author, chengxiang.zhuge@polyu.edu.hk)

# Abstract

This paper developed a data-driven micro-simulation optimization model to deploy charging infrastructure for a large-scale electric bus network, considering both traditional charging posts and wireless charging lanes (WCLs). The optimization model has two objectives: 1) minimize the total system cost and 2) maximize the level of service. We used New York City as the study area, and one-day GPS trajectories of 3,133 buses were analyzed to develop the micro-simulation approach, so as to represent the bus operation well. The results showed that the scenario with both charging posts and WCLs deployed had a significantly higher level of service (with its total delay time being 48.11% shorter), more energy saved and fewer emissions than the scenario with only charging posts deployed, though its total cost was 0.76% higher. Moreover, the sensitivity analysis results show that the parameters associated with electric buses and charging facilities could heavily influence the outputs of interest.



**Keywords:** Electric Bus; Trajectory Data; Wireless Charging; Micro-simulation Approach

# 1 Introduction

As one of the key components of Sustainable Development Goals (SDGs), there is an urgent international call for close cooperation, and global greenhouse gas emissions should be reduced to zero by 2050 (United Nations, 2022). Transportation industry was responsible for 37% of all worldwide carbon emissions in 2021 (IEA, 2022). Electric Vehicles (EVs) are gaining popularity as viable alternatives to traditional vehicles (e.g., petrol cars) in order for the achievement of Net-zero commitments in the transport sector (United Nations Environment Programme, 2022). The automotive industry, academia, and the public transit sector have all shown considerable interest in electrifying modes of transportation (Chen, Yin, & Song, 2018; Wang, Liao, & Lu, 2022).

Buses powered by traditional internal combustion engines (ICE) are a major contributor to road pollution in most cities (Jaiprakash, Habib, Kumar, Sharma, & Haider, 2017). The public transportation department of the government has been shifting toward more environmentally friendly fuel sources like electricity in an effort to lessen local air pollution caused by gasoline and diesel-powered buses (Topal & Nakir, 2018). Electric buses (E-buses), powered by electricity, have the potential to lessen environmental impacts, including noise and air pollution (Eda et al., 2016).

The electrification of transportation systems, particularly the bus system, depends

heavily on the availability of charging facilities (Zhuge & Shao, 2018). For bus operators, they need to make a trade-off between the cost of charging facilities and charging efficiency (which could influence the operational efficiency of the whole bus system). Therefore, this paper attempts to explore the suitability of advanced charging facilities, i.e., wireless charging lanes (WCLs). WCLs allow E-buses to receive power as they go along the lanes based on the dynamic wireless charging (DWC) technology, which can transfer electric energy remotely from the transmitting coils beneath the lanes to the receiving coils on the chassis of E-buses when E-buses travel on WCLs (Buja, Bertoluzzo, & Dashora, 2016). Therefore, WCLs could significantly reduce the demand for battery size, save charging time and improve the operational efficiency of the electrified bus network. In practice, many cities, such as Sejong, Madrid and Tel Aviv, have deployed WCLs for E-buses operations in recent years. For example, the Korean Institute of Advanced Technology (KAIST) has studied DWC since 2009 and developed the On-Line Electric Vehicle (OLEV) system, which was the first commercialized WCL system for E-buses in the world (Machura & Li, 2019). Sweden officially authorized a standard for WCLs in November 2022 and planned to put the first WCL (with about 0.9 million dollars per km for two-way two-lane road) into practice in 2026, which is expected to reduce cost by about 52 billion dollars annualized due to the need for a smaller battery size (Swedish Electromobility Centre, 2019). These application cases show that the costs associated with equipment like coils, charging pads, and inverters would make WCLs more costly than traditional charging facilities, but WCLs could significantly cut the upfront battery cost by decreasing the battery size

required of E-buses.

In order for a better charging facility deployment plan, we develop a data-driven large-scale simulation-based optimization model for deploying both traditional charging posts and WCLs, using real-world bus trajectory data collected from a citywide bus network in New York City (NYC). In previous EV studies, such data-driven micro-simulation approaches have seldom been developed for large-scale real-world scenarios.

# 2 Literature Review

Most studies on the deployment of charging facilities for E-buses were mainly centered on traditional charging stations rather than WCLs. Therefore, we will first review recent models for deploying charging stations in Section 2.1, and then review models for deploying WCLs in Section 2.2.

## 2.1 Deploying Charging Stations for Electric Bus Systems

Previous optimization models for deploying charging stations looked at four key elements in the system, namely, charging stations/posts, battery capacities (most studies assumed that all E-buses or the E-buses served for one route have the same battery capacity), vehicle fleet size, and charging schedules. For instance, He, Song, and Liu (2019) optimized the charging schedules and management (i.e., restrictions on charging durations); Hsu, Yan, and Huang (2021), Lee, Shon, Papakonstantinou, and Son (2021)

and Wang et al. (2022) optimized the allocation of stations, battery capacity and fleet size; Liu, Qu, and Ma (2021), Zhou, Wang, Wang, and Li (2022) and He, Liu, and Song (2022) optimized the allocation of stations, battery capacity and charging schedules. Most studies assumed that charging posts (i.e., charging power) at all charging stations are the same, or each station only has one type of charging post (i.e., charging power). Recently, some attempts have been made to deploy fast charging stations for E-buses (He, Liu, & Song, 2020; He et al., 2019; Wu et al., 2021), which are expected to reduce charging time and further improve the operational efficiency of the bus system.

In terms of model structures, two main model types with a single optimization objective have been widely used to formulate the deployment problem, including single objective optimization based on mixed integer linear programming (MILP) (Chen, Atasoy, Robenek, Bierlaire, & Thémans, 2013; Xylia, Leduc, Patrizio, Kraxner, & Silveira, 2017; Zhou et al., 2022), and mixed integer nonlinear programming (MINLP) (He et al., 2020, 2022; Liu et al., 2021). For example, Zhou et al. (2022) designed a joint MILP and robust optimization model to optimize the number of chargers at bus terminals, charging schedule, and battery capacities with the aim of minimizing the cost. He et al. (2020) proposed a MINLP model to optimize the charging schedule and management at fast charging stations, and then reformulated the model as a linear program using a discretizing approach and a linear reformulation methodology.

In general, the objectives of these optimization models focused on the weighted sum of different kinds of cost, including the charging station manufacturing cost, vehicle

cost, and battery cost. Based on this, the electricity consumption cost (He et al., 2020; Lee et al., 2021; Xylia et al., 2017), the operation cost of charging stations (Hsu et al., 2021; Uslu & Kaya, 2021), passenger waiting time cost (Liu et al., 2021; Rogge, van der Hurk, Larsen, & Sauer, 2018) are also considered in the weighted sum. In addition, Uslu and Kaya (2021) also proposed an optimization model to minimize the number of stops on the routes of the buses to reduce passenger confusion.

These charging station location optimization models were mostly tested in small-scale real-world bus networks, such as eight routes and 36 routes in downtown Salt Lake City (He et al., 2020; He et al., 2019), 13 routes in Taoyuan City (Hsu et al., 2021), one route in Seogwipo-city (Lee et al., 2021), 11 routes in Beijing (Liu et al., 2021), four routes in Oslo (Wang et al., 2022), five routes in Singapore (Zhou et al., 2022), and six routes in Salt Lake City (He et al., 2022). Some attempts have been made to test the optimization models in large-scale real-world bus networks. For example, Xylia et al. (2017) tested the optimization framework by real-world 526 bus routes in Stockholm; Uslu and Kaya (2021) tested the MILP of station deployment through a bus network with 332 routes in Turkey. However, few of them used real-world operation data (e.g., GPS bus trajectory data) for model development or testing.

## 2.2 Deploying Wireless Charging Lanes (WCLs)

Many facility allocation models have been developed to deploy WCLs (see Table A.1 in Appendix A for a summary of existing literature). Some of them were particularly for

E-buses, mainly based on nonlinear programming (NLP), mixed integer linear programming (MILP), robust optimization, or bi-level operation methods. For example, Jang, Suh, and Kim (2016) proposed a MILP model to allocate the WCLs and optimize the battery capacity for one real-world bus route in Korea to minimize the cost of batteries and WCLs. Mouhrim, Alaoui, and Boukachour (2016) proposed a WCL deployment optimization model based on NLP to minimize the cost of bus batteries and WCLs. Liu and Song (2017) proposed a robust optimization model of deploying the WCLs and optimizing the battery capacity to minimize the cost of batteries and WCLs, and tested the model through eight real-world bus route network. Alwesabi, Liu, Kwon, and Wang (2021) designed a MILP framework to optimize the allocation of WCLs, battery capacity (one size), and bus fleet size with the aim of minimizing the costs of WCLs, batteries and vehicles.

These facility allocation models used different optimization objectives. Most of the studies aimed to minimize the manufacturing cost of WCLs, and several studies also considered minimizing some other costs (e.g., the cost of batteries, the travel time cost, or the energy consumption or greenhouse emissions), or maximizing the EV flow captured by WCLs or the recharged electricity. For example, Ushijima-Mwesigwa, Khan, Chowdhury, and Safro (2017) proposed an NLP deployment model to maximize the number of EVs captured by WCLs or maximize the recharged electricity. Ngo, Kumar, and Mishra (2020) built a bi-level optimization deployment framework to minimize travel time or energy consumption. Liu, Zou, Chen, and Long (2021)

proposed a bi-level method to minimize the weighted cost of travel time and WCLs. This indicates that the optimization objectives are threefold: facility cost, travel time cost, and energy consumption.

These facility location models were mostly applied into small-scale numerical hypothetical examples. For example, Zhang, Rey, and Waller (2018) used the Sioux Falls network to test the proposed bi-level optimization framework for charging post and WCL deployment. Iliopoulou and Kepaptsoglou (2019) created a new bus network and WCL deployment plan to test the feasibility of their bi-level optimization model in a benchmark network (30 nodes and 90 links). Some of the models have been applied into small-scale real-world scenarios with one or multiple bus routes. For example, Jang et al. (2016) attempted to deploy WCLs for one bus route based on its timetable and route direction. Hwang, Jang, Ko, and Lee (2018) deployed WCLs for a real-world bus network with five routes in Korea based on MILP. Alwesabi, Wang, Avalos, and Liu (2020) optimized the allocation of WCLs and battery size for the off-campus college transportation system at Binghamton University with six bus routes based on MILP. In addition, some studies also used the real-world road network to test the models. For example, Wang, Yang, Chen, and Guan (2019) used traffic characteristics of signal-controlled intersections extracted from the taxi trajectory data in Shanghai to provide statistical rules to deploy the WCLs for EVs, including E-buses.

## 2.3 Research Gaps and Aims

As reviewed above, various optimization models have been developed to deploy traditional charging stations for E-buses. Recently, some attempts have also been made to deploy wireless charging lanes (WCLs), as they are expected to save charging time and further improve the operational efficiency of the electrified bus network. However, it remains unclear the extent to which these WCLs could improve operational efficiency, and whether the cost would be acceptable. In response, this paper develops a bi-objective optimization model to deploy both traditional charging stations/posts and WCLs. With the model, we are able to explore the technical and economic suitability of deploying WCLs in an electrified bus network. In particular, we use dedicated bus lanes as candidates for WCLs, so as to reduce the impacts of WCLs on the traffic system. In terms of methodology, we develop a data-driven simulation-based optimization approach for deploying charging infrastructure on a large-scale electrified bus network, using real-world bus trajectory data in New York City (NYC). Such data-driven micro-simulation approaches are expected to better represent the real bus operation, so as to better calculate charging demand at the micro-scale, which is essential for deploying charging infrastructure. However, such data-driven approaches have seldom been developed for a citywide electrified bus network in the real world.

# 3 Study Area and Data Sources

## 3.1 Study Area: New York City (NYC)

New York City (NYC) was used as the study area as it has lots of open datasets for model development, such as bus trajectory data, bus timetables, road networks, etc. NYC is the center of the New York metropolitan area with a dense population in the United States. NYC's bus service is the largest in North America (Port Auyhority NYNJ, 2008).

NYC is introducing electric buses into its fleet quickly (Andrew Catania, 2019). The government aimed to entirely electrify its bus network by 2040, but the bus fleet only had 15 electric buses for two bus routes by April 2022 (Authority, 2021; Kessler, 2022; Metropolitan Transportation Authority Bus Company, 2021). One of the main barriers is still the lack of charging facilities (NYC Department of Transportation, 2021). Therefore, there is an urgent need to rationally plan charging facilities for a future fully electrified bus network.

## 3.2 Data Sources

Three main datasets will be used to develop the data-driven simulation-based optimization model for deploying charging facilities in NYC, including the real NYC bus operation data, the road network, and the layout of dedicated bus lanes. Fig. 1 shows the bus routes and dedicated bus lanes.

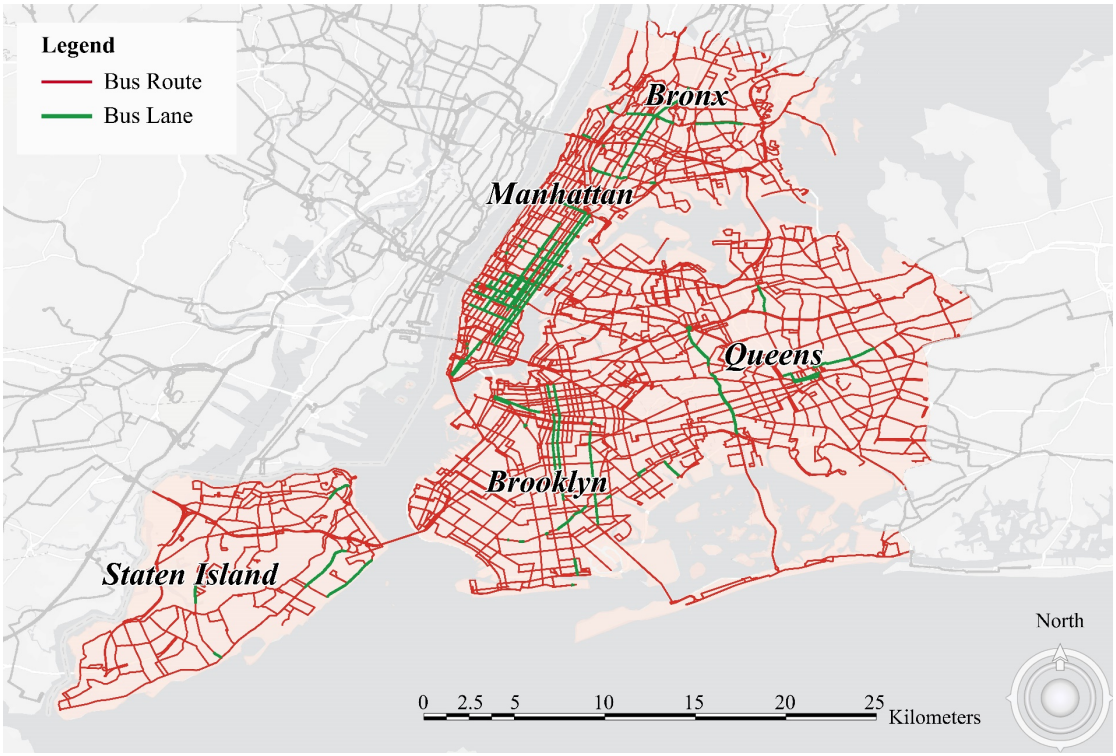


Fig. 1 Bus Routes and Dedicated Bus Lanes in New York City (Data sources: OpenStreetMap (2021); NYCOpenData (2021); Michael (2017))

**(1) The NYC road network**

The road network with 213,218 links was obtained from OpenStreetMap (OpenStreetMap, 2021). The dataset contains road information and topology, such as node ID of the links' endpoint and the length of each link. It is worth noting that each road consists of several links in the road network data. The average length of all road links is 17.5 meters, which is relatively short. Thus, it would be acceptable to assume in the simulation that buses move at a constant speed on each road link. Therefore, we calculated the average speed of buses traveling on each link based on the bus trajectory data, which was used as the model's input data (see Section 4.5).

**(2) The real NYC bus operation data**

The data was provided by Stone Michael (Michael, 2017), a solutions architect at Telstra. Specifically, the data contains the bus network, route, timetable, as well as real GPS trajectory data on 1st December 2017 (Friday). After data cleaning and map-matching (see Appendix B for more details), a dataset containing 3,133 buses (with a sample rate of 95.03%) for 310 routes was obtained. The total operating mileage of the bus network was 9,700 kilometers.

Based on the analysis of the bus trajectory data, we can find spatial patterns of the moving buses on the road network (see Fig. 2): essentially, the bus density on the dedicated bus lanes tended to be higher than the other general lanes. At the borough level, Manhattan, central Queensland, and eastern Brooklyn had more moving buses than the other areas.

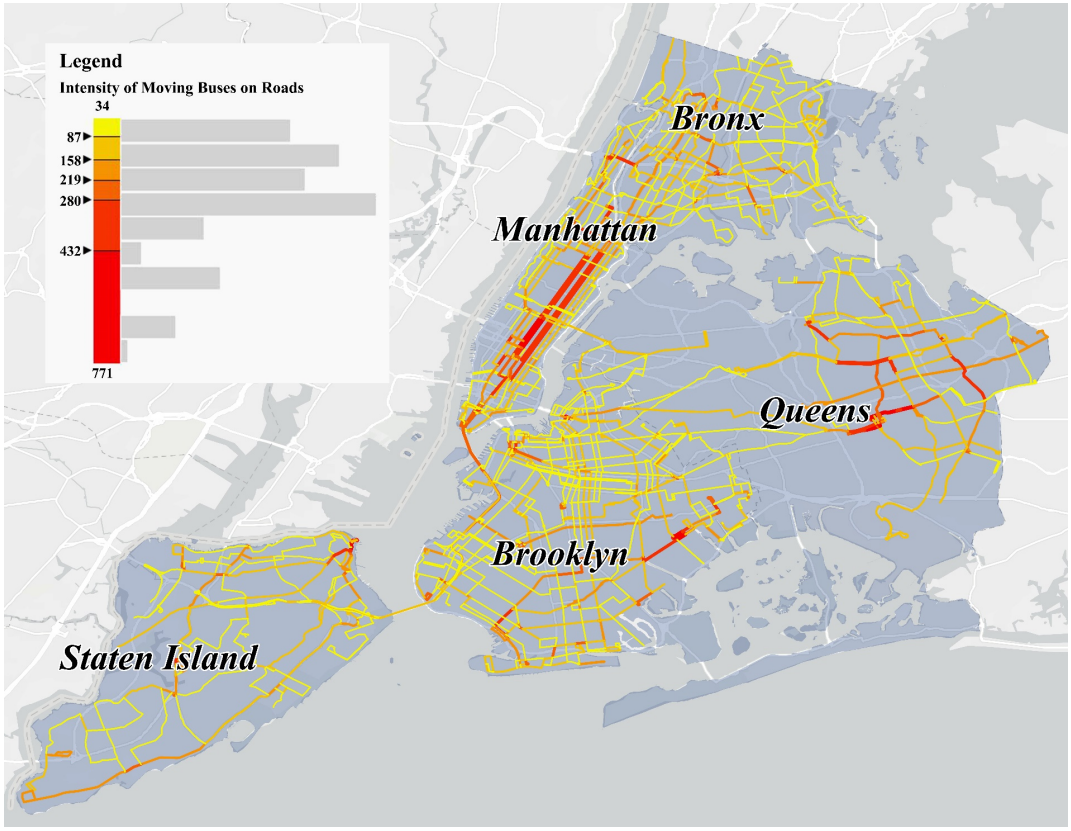


Fig. 2 Intensity of Moving Buses on the Road Network (extracted from the bus trajectory data)

Fig. 3 illustrates the temporal distribution of the moving buses by the hour. There were two peak periods, namely 7:00-10:00 and 14:00-18:00. This indicated a typical commuting pattern of citizens on a working day.

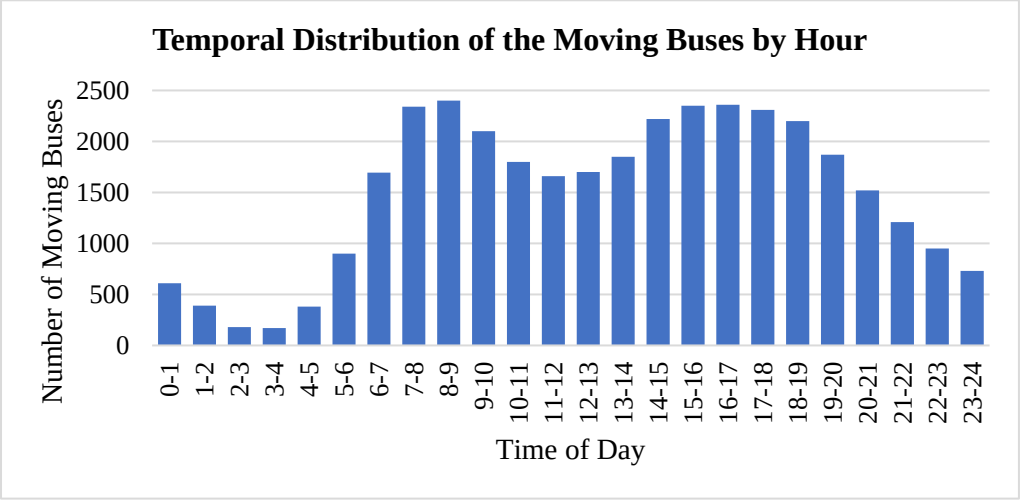


Fig. 3 Temporal Distribution of the Moving Buses by the Hour

**(3) The layout of dedicated bus lanes in NYC**

NYC had several dedicated bus lanes with a total length of 222.7 km (until May 2021). The layout of bus lanes was collected from the NYCOpenData (2021). In total, 10,776 bus lane links will be used in this study as candidates for WCLs (see Section 4.1).

# 4 Methodology

## 4.1 Problem Description

One of the critical issues facing bus electrification is the choice and deployment of different types of charging facilities, including both traditional and advanced charging facilities, as they have their own pros and cons (e.g., fast charging speed but high cost). As the most popular charging facilities nowadays, charging stations supply electricity through charging posts with different power rates, which can be generally grouped into fast and slow charging ones. Apart from traditional charging posts, some advanced charging facilities, such as wireless charging lanes (WCLs), have received growing attention. They allow electric buses (E-buses) to get recharged with a fixed output power by the transfer pads underneath the roads. Next, we introduce how we designed scenarios, made model assumptions, and generated candidate locations for charging facilities in solving the problem.

**(1) Scenario Design**

To help bus operators to choose between different charging facilities, we developed a data-driven simulation-based bi-objective optimization approach (see Fig. 4 in Section 4.2.1) to deploy charging facilities using real-world bus trajectory data as one of the inputs. In particular, the approach can deal with the following two scenarios with different charging facilities given:

**Scenario A**: only charging stations with fast and slow charging posts are available.

**Scenario B**: both WCLs and charging stations are available.

During the optimization process, the operation of the E-bus system is simulated with the real data. Specifically, we assumed that the original bus routes remain in the electrified bus system. In other words, the bus trajectories were the same in the three scenarios with conventional vehicles (baseline scenario), E-bus and charging station (Scenario A), and E-bus, charging station and WCL (Scenario B), when the buses travel from start to end bus stops, following the pre-defined routes and timetable. Here, when simulating E-buses charging at stations, the charging behavior occurs only in the idle time between two tasks (loops) under the timetable constraints; when simulating E-buses charging on WCL, the charging behavior does not affect the travel speed due to the timetable constraints.

**(2) Model Assumptions**

We also make the following key assumptions in the model:

- All buses are electrified with an optimal battery capacity (i.e., one of the decision variables in the model) based on battery type candidates.

- An E-bus can serve multiple bus routes.

- All E-buses have got fully charged prior to their departure for their first task, as they should have sufficient charging after getting recharged overnight.

**(3) Candidate Locations for Charging Facilities**

In terms of charging stations, charging events are expected to occur in the idle time between two tasks (loops), as mentioned above, which means that the candidate locations are closely related to where the E-bus starts and ends a task (loop). Based on mining the real bus GPS trajectory data, we found several clusters of start/end bus stops. Therefore, each cluster was considered as a candidate location for a charging station, in order to serve more E-buses.

In terms of WCLs, we used dedicated bus lanes as candidate locations. On the one hand, these candidate locations would help to reduce a negative impact on the traffic system (He, Yang, Tang, & Huang, 2020) since there is no need to occupy additional road space (or lanes) for WCLs. On the other hand, WCLs are costly and would thus be better to be deployed on those road links with more buses. Therefore, dedicated bus lanes would be good candidates for WCLs, as they tend to serve more buses (see Fig. 2).

Table 1 summarizes all the notations used in the model, and the last column indicates how the variables will be parameterized where applicable.

Table 1 Notations used in the Model

| Symbol | Description | Source |
|---|---|---|
| $G(N, L)$ | Set of road network with index $(n, l)$, where $N, L$ denote nodes/intersections and links, respectively | N.A. |
| $(i, j)$ | Node pair denotes link $L$, $i, j \in N, i \neq j$ | N.A. |
| $d_{ij}$ | Length of $(i, j)$ (kilometer) | Road network data |
| $t_{ij}$ | Average travel time of $(i, j)$ (hour) | Bus operation data |
| $h_{ij}$ | Elevation differences of $(i, j)$ (°) | N.A. |
| $w_{ij}$ | Weather parameters of $(i, j)$ | Input by Users |
| $K$ | Set of E-bus routes with index $k$ | Bus operation data |
| $O_k$ | Origin of E-bus route $k$ | Bus operation data |
| $D_k$ | Destination of E-bus route $k$ | Bus operation data |
| $L_k$ | Set of links with E-buses running, $L_k \subset L$ | Bus operation data and road network data |
| $N_k$ | Set of nodes with E-buses running, $N_k \subset N$ | Bus operation data and road network data |
| $H_k$ | Departure frequency (i.e., total loops) of E-bus route $k$ in a day with index $h_k$ | Bus operation data |
| $P$ | Set of E-buses with index $p$ | Bus operation data |
| $e_{p,k,h,i}$ | State of charge (SOC) of $p$ E-bus in $i$ node during $h_k$ loop (kWh) | N.A. |
| $e_{p,k',h+1,O_k}$ | SOC of $p$ E-bus after $h_k$ loop and getting charged, i.e., the SOC at the point when $p$ E-bus starts the next loop (kWh) | N.A. |
| $\triangle e_{p,k,h,i,j}$ (negative) | Electricity consumption of $p$ E-bus between $(i, j)$ link during $h_k$ loop (kWh) | N.A. |
| $M$ | Set of charging stations with index $m$ | Design Variable |
| $X_{f,m}$ | Number of fast charging posts at charging station $m$ with index $x_{f,m}$ | Design Variable |
| $X_{s,m}$ | Number of slow charging posts at charging station $m$ with index $x_{s,m}$ | Design Variable |
| $a_f$ | Charging power of fast charging posts (kW) | Input by Users |
| $a_s$ | Charging power of slow charging posts (kW) | Input by Users |
| $Eff_f^{Sta}$ | Charging efficiency of fast charging post (%) | Input by Users |
| $Eff_s^{Sta}$ | Charging efficiency of slow charging post (%) | Input by Users |

| Symbol | Description | Source |
|---|---|---|
| $t_{p,k,h,m,f}$ | Actual charging duration of $p$ E-bus using fast charging post at station $m$ after $h_k$ loop (hour) | N.A. |
| $t_{p,k,h,m,s}$ | Actual charging duration of $p$ E-bus using slow charging post at charging station $m$ after $h_k$ loop (hour) | N.A. |
| $\triangle e_{p,k,h,m}$ (positive) | The SOC of $p$ E-bus charged at charging station $m$ after $h_k$ loop (kWh) | N.A. |
| $T_{(m,k,p,h,ar)}$ | Time when E-bus $p$ arrives at station $m$ after $h_k$ loop | N.A. |
| $T_{(m,k,p,h,st)}$ | Time when E-bus $p$ starts charging after $h_k$ loop at station $m$ | N.A. |
| $T_{(m,k,p,h,fs)}$ | Time when E-bus $p$ is fully charged or time when E-bus $p$ is charged to have enough electricity for the next loop after $h_k$ loop at station $m$ | N.A. |
| $T_{(m,k,p,h,sp)}$ | The latest time when E-bus $p$ needs to leave station $m$ after $h_k$ loop because of the time limit for the next loop | Bus operation data |
| $t_{(m,k,p,h,sy)}$ | Duration that E-bus $p$ stays at station $m$ after $h_k$ loop (hour) (considering both waiting and charging times) | N.A. |
| $t_{(m,k,p,h,pl)}$ | Charging duration of E-bus $p$ at station $m$ after $h_k$ loop (hour) | N.A. |
| $t_{(m,k,p,h,ps)}$ (positive or negative) | Delay time of E-bus $p$ at station $m$ after $h_k$ loop (hour) | N.A. |
| $T_{m,x_{f\ or\ s,m},p',h_k,fs}$ | Time when charging post $x_{f\ or\ s,m}$ finishes serving the last E-bus $p'$ after $h_k$ loop at station $m$ | N.A. |
| $t_{delay}$ | Total delay time of all E-buses (hour) | N.A. |
| $T^{bat}$ | Lifespan of a battery (year) | Input by Users |
| $c_p$ | Battery capacity of $p$ E-bus (kWh) | Design Variable (with battery type candidates input by users for selection) |
| $C^{bat}$ | Battery cost (per-unit) ($/kWh) | Input by Users |
| $COST^{bat}$ | Total cost of all batteries ($) | N.A. |
| $C^{veh}$ | Vehicle cost (without battery cost) (per-unit) ($/vehicle) | Input by Users |
| $COST^{veh}$ | Cost of all vehicles (without battery cost) ($) | N.A. |
| $T^{veh}$ | Lifespan of a vehicle (year) | Input by Users |
| $C^{sta,m}$ | Station manufacturing cost (per-unit) ($/station) | Input by Users |
| $COST^{sta,m}$ | Total manufacturing cost of all stations ($) | N.A. |

| Symbol | Description | Source |
|---|---|---|
| $C^{sta,o}$ | Staff cost and station equipment consumption cost of a charging station ($/year) | Input by Users |
| $T^{sta}$ | Lifespan of charging station (year) | Input by Users |
| $COST^{sta,o}$ | Total operating cost of all stations ($) | N.A. |
| $C^{pos}$ | Post manufacturing cost (per-unit) ($/kW) | Input by Users |
| $COST^{pos}$ | Total manufacturing cost of all posts ($) | N.A. |
| $d_{i,j}^{WCL}$ | =0 if no wireless charging lane on $(i,j)$ link<br>=Length of wireless charging lane on $(i,j)$ link (kilometer) otherwise | Design Variable |
| $t_{i,j}^{WCL}$ | =0 if no wireless charging lane on $(i,j)$ link<br>=Travel time on wireless charging lane on $(i,j)$ link (hour) otherwise | N.A. |
| $a_{WCL}$ | Charging power of wireless charging lane (kW) | Input by Users |
| $Eff^{WCL}$ | Charging efficiency of wireless charging lane (%) | Input by Users |
| $\triangle e_{p,k,h,i,j}^{WCL}$ (non-negative) | =0 if no wireless charging lane on $(i,j)$ link<br>=SOC of $p$ E-bus obtained on wireless charging lane on $(i,j)$ link after $h_k$ loop (kWh) otherwise | N.A. |
| $T^{WCL}$ | Lifespan of wireless charging lane (year) | Input by Users |
| $COST^{WCL}$ | Total manufacturing cost of all wireless charging lane cost ($) | N.A. |
| $C^{WCL}$ | Wireless charging lane cost (per-unit) ($/kilometer) | Input by Users |
| $m_1, m_2, m_3, m_4, b$ | Parameters that affect the energy consumption of E-bus by weather, elevation, travel time and travel distance, respectively | Input by Users |
| $C^{ele}$ | Electricity cost (per-unit) ($/kWh) | Input by Users |
| $COST^{ele}$ | Total electricity cost per day ($) | N.A. |
| $C^{driver}$ | A driver's service fee per day (per-unit) ($/driver/day) | Input by Users |
| $COST^{driver}$ | Total drivers' service fee per day ($) | N.A. |

## 4.2 Bi-objective Optimization Model based on Data-driven Micro-simulation

### 4.2.1 Model Overview

Fig. 4 shows the overview of the data-driven micro-simulation-based bi-objective

optimization approach. This optimization model consists of three key components, including two objectives (see Section 4.2.2 for details), four constraints (see Section 4.2.3 for details) and three connected sub-models (see Section 4.3-4.5 for details), as shown in Fig. 4-(a). In the two scenarios defined in Section 4.1 (i.e., Scenario A - only Charging Station and Scenario B - Charging Station & WCL), we will use this approach to find the optimal solutions for deploying charging facilities.

Time-driven and event-driven simulations are two typical approaches that have been widely used to simulate bus system operation (Abdelwahed, van den Berg, Brandt, Collins, & Ketter, 2020; Wang et al., 2022). This study used the event-driven simulation approach due to its high flexibility (Meyer, 2014). Specifically, the simulation was focused on the three key types of discrete events, namely queuing, fuel consumption, and E-bus charging events, which were dealt with by the three connected models, respectively (see Section 4.3-4.5). During the simulation, events are processed one by one with the three steps below in sequence: 1) check the stop criteria of the simulation system (e.g., whether all E-buses finish the transport tasks), which are used to decide whether to stop the simulation; 2) take the first event off the event list and process it. Here, the event list is composed of a series of events which are sorted by time, including queuing, fuel consumption, and E-bus charging events; 3) update the time of the simulation system according to the event being processed.

To better reflect the real-world situations (e.g., traffic congestion) and consider the stochasticity effect observed in road traffic dynamics, a data-driven approach was used

to simulate the bus operation. Specifically, we extracted the relevant information from real bus GPS trajectory data, which can well consider the realistic traffic scenes, including the time-dependent travel speed of each bus on each road link and departure and arrival times of each trip. This real-world information can be used to generate the three key events in the simulation, namely queuing and delay (see Section 4.3), electricity consumption (see Section 4.4), and charging behavior at stations and on WCLs (see Section 4.5).

The data flow (see Fig. 4-(b)) shows how different real-world information from different datasets was combined and further used in the simulation after data cleaning (as detailed in Section 3.2) and map-matching (i.e., linking bus trajectories to road links where buses are moving). As shown by the colored arrows for data flows in Fig. 4-(b), we analyzed the bus trajectory data to extract travel and parking behaviors for developing the simulation of E-bus's possible queuing and charging at a charging station (sub-model 1), the simulation of E-bus's electricity consumption (sub-model 2), and the simulation of E-bus's charging events (sub-model 3). Here, the other datasets, including the bus network, timetables, road network and layout of dedicated bus lanes, are also needed for the implementation of these data-driven sub-models.

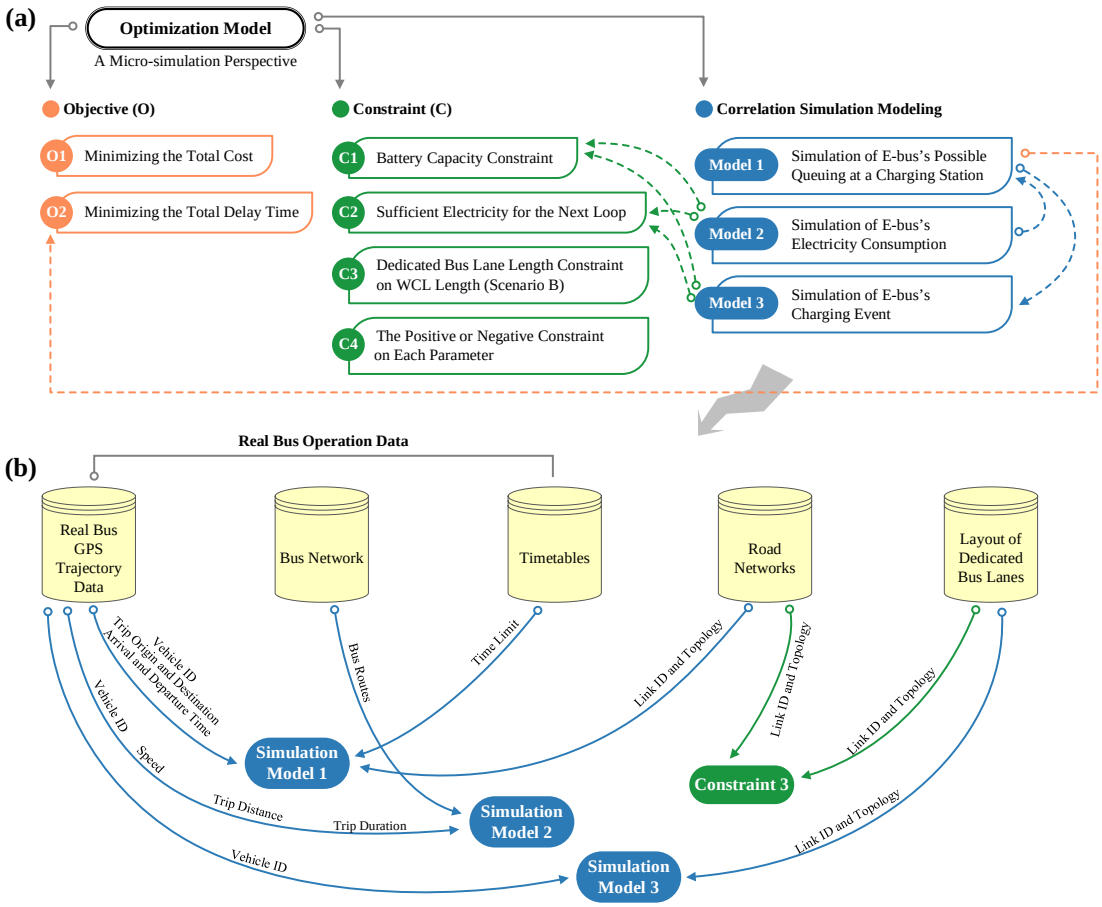


Fig. 4 Micro-simulation-based Bi-objective Optimization Approach. (a) Key Components of the Model; (b) Data Flow of the Data-Driven Micro-simulation

## 4.2.2 Objective Functions

From the perspective of bus operators, they need to make a trade-off between the total cost of deploying charging facilities and the level of service that they want to maintain. We mathematically described this trade-off as a bi-objective optimization model as follows:

**Objective 1: minimizing the total cost of the E-bus system**

As aforementioned, the optimization model will be used to deal with two typical

scenarios, namely Scenario A with charging stations only and Scenario B with both charging stations and WCLs. Therefore, Objective 1 ( $Z_1^A$ and $Z_1^B$ ) can be mathematically described by Equations (1A) and (1B) for Scenarios A and B, respectively. To evaluate the cost per unit of time, we consider the lifespan of the E-bus battery ($T^{bat}$), E-bus vehicle ($T^{veh}$), charging station ($T^{sta}$), and WCL ($T^{WCL}$).

$$\begin{aligned} Z_1^A &= Min\ COST \\ &= Min\left(\frac{COST^{bat}}{T^{bat}} + \frac{COST^{veh}}{T^{veh}} + \frac{COST^{sta,m} + COST^{pos}}{T^{sta}}\right. \\ &\left. + COST^{sta,o}\right) \times \frac{1}{365} + COST^{ele} + COST^{driver} \end{aligned} \tag{1A}$$

$$\begin{aligned} Z_1^B &= Min\ COST \\ &= Min\left(\frac{COST^{bat}}{T^{bat}} + \frac{COST^{veh}}{T^{veh}} + \frac{COST^{sta,m} + COST^{pos}}{T^{sta}}\right. \\ &\left. + COST^{sta,o} + \frac{\boldsymbol{COST^{WCL}}}{\boldsymbol{T^{WCL}}}\right) \times \frac{1}{365} + COST^{ele} \\ &+ COST^{driver} \end{aligned} \tag{1B}$$

**Scenario A: only charging station**

In Scenario A, the total cost includes the E-bus battery cost ($COST^{bat}$), vehicle cost (without battery cost) ( $COST^{veh}$ ), the manufacturing cost of charging stations ($COST^{sta,m}$), operating cost of charging stations ($COST^{sta,o}$) (including staff service fee and equipment consumption cost), the manufacturing cost of charging posts ($COST^{pos}$), electricity cost ($COST^{ele}$), and driver service fee ($COST^{driver}$). They can be calculated by Equations (2)-(8), respectively. It is worth noting that the reason for

separating vehicle cost (without battery cost) and battery cost is to investigate the direct effect of battery size on the model.

$$COST^{bat} = \sum_{p \in P} c_p \times C^{bat} \tag{2}$$

$$COST^{veh} = P \times C^{veh} \tag{3}$$

$$COST^{sta,m} = M \times C^{sta,m} \tag{4}$$

$$COST^{sta,o} = M \times C^{sta,o} \tag{5}$$

$$COST^{pos} = C^{pos} \times \left( \sum_{m \in M} X_{f,m} \times a_f + X_{s,m} \times a_s \right) \tag{6}$$

$$COST^{ele} = C^{ele} \times \left( a_f \times \sum_{p \epsilon P} t_{p,k,h,m,f} + a_s \times \sum_{p \epsilon P} t_{p,k,h,m,s} \right) \tag{7}$$

$$COST^{driver} = P \times C^{driver} \tag{8}$$

where $COST^{bat}$ is related to each battery's capacity ($c_p$) and the unit battery cost in kWh ($C^{bat}$). $COST^{veh}$ is related to the number of E-buses ($P$) and the unit vehicle cost without battery cost ($C^{veh}$). $COST^{sta,m}$ is related to the number of charging stations ($M$) and the unit station manufacturing cost ($C^{sta,m}$). $COST^{sta,o}$ is related to the number of charging stations ($M$) and the unit station staff and equipment consumption cost ($C^{sta,o}$). $COST^{pos}$ is related to the unit post manufacturing cost in kW ($C^{pos}$), the fast and slow charging post's charging power ($a_f$ and $a_s$), and the numbers of fast and slow charging posts ($X_{f,m}$ and $X_{s,m}$). $COST^{ele}$ is related to the unit electricity cost in kWh ($C^{ele}$), the

fast and slow charging post's charging power ($a_f$ and $a_s$), and the charging duration using fast and slow charging posts ($t_{p,k,h,m,f}$ and $t_{p,k,h,m,s}$). $COST^{driver}$ is related to the number of E-buses ($P$) and a driver's service fee per day ($C^{driver}$).

**Scenario B: charging station and WCL**

In Scenario B, we also need to consider the costs related to WCL on top of Scenario A: the electricity cost ($COST^{ele}$) is calculated by Equation (9) instead, and the manufacturing cost of WCLs ($COST^{WCL}$) is calculated by Equation (10).

$$COST^{ele} = C^{ele} \times \left( a_f \times \sum_{p \epsilon P} t_{p,k,h,m,f} + a_s \times \sum_{p \epsilon P} t_{p,k,h,m,s} + \sum_{i \epsilon N} \sum_{j \epsilon N} t_{i,j}^{WCL} \times a_{WCL} \right) \quad (9)$$

$$COST^{WCL} = C^{WCL} \times \sum_{i \epsilon N} \sum_{j \epsilon N} d_{i,j}^{WCL} \quad (10)$$

Here, based on Equation (7), Equation (9) adds the electricity cost of WCL, which is related to the unit electricity cost in kWh ($C^{ele}$), the WCL's charging power ($a_{WCL}$), and the charging duration using WCLs ($t_{i,j}^{WCL}$). $COST^{WCL}$ is related to the unit WCL manufacturing cost in kilometer ($C^{WCL}$) and the length of WCL ($d_{i,j}^{WCL}$).

**Objective 2: minimizing the total delay time of the E-bus operation system**

To maintain a high level of service for the whole bus system, we include Objective 2

($Z_2$) in the optimization, which is to minimize the total delay time ($t_{delay}$), as shown by Equation (11). The total delay time ($t_{delay}$) is the sum of the delay time ($t_{(m,k,p,h,ps)}$) of all E-buses on all routes at all charging stations.

$$Z_2 = Min\ t_{delay} = Min - \sum_{k\in K}\sum_{h_k\in H_k}\sum_{p\in P}\sum_{m\in M} t_{(m,k,p,h,ps)} \quad , t_{(m,k,p,h,ps)} < 0 \tag{11}$$

where $t_{(m,k,p,h,ps)}$ is calculated by Equation (18) in Section 4.3.

### 4.2.3 Constraints

The constraints of the optimization model include:

**Constraint 1:** The state of charge (SOC) of an E-bus ($e_{p,k,h,i}$) should not be larger than its capacity ($c_p$) at any time, including 1) at the time when E-bus is getting charged on WCLs (as shown in Equation 12), and 2) at the time when E-bus finishes charging at a charging station (as shown in Equation 13A for Scenario A and Equation 13B for Scenario B).

$$0 \le e_{p,k,h,i} \le c_p \tag{12}$$

$$e_{p,k',h+1,O_k} = e_{p,k,h,O_k} + \sum_{i\in N}\sum_{j\in N} \triangle\, e_{p,k,h,i,j} + \triangle\, e_{p,k,h,m} \le c_p \tag{13A}$$

$$e_{p,k',h+1,O_k} = e_{p,k,h,O_k} + \sum_{i\in N}\sum_{j\in N} \triangle\, e_{p,k,h,i,j} + \sum_{i\in N}\sum_{j\in N} \triangle\, e^{WCL}_{p,k,h,i,j} + \triangle\, e_{p,k,h,m} \le c_p \tag{13B}$$

where the electricity consumption of $p$ E-bus between $(i, j)$ link during $h_k$ loop ($\triangle e_{p,k,h,i,j}$) is calculated by Equation (21) in Section 4.4, the SOC of $p$ E-bus charged at charging station $m$ after $h_k$ loop ($\triangle e_{p,k,h,m}$) is calculated by Equation (22) in Section 4.5, and the SOC of $p$ E-bus obtained on the wireless charging lane on $(i, j)$ link after $h_k$ loop ($\triangle e^{WCL}_{p,k,h,i,j}$) is calculated by Equation (23) in Section 4.5.

**Constraint 2:** After a charging event finishes, the SOC of an E-bus should be sufficient for the next loop. In Scenario A, after an E-bus finishes charging at a station, the SOC should satisfy Equation (14A). In Scenario B, this constraint also needs to consider the electricity obtained on the WCL ($\triangle e^{WCL}_{p,k',h+1,i,j}$), which means E-bus may get charged during the loop, as shown by Equation (14B).

$$e_{p,k',h+1,O_k} \geq -\sum_{i\in N}\sum_{j\in N} \triangle e_{p,k',h+1,i,j} \tag{14A}$$

$$\begin{aligned} e_{p,k',h+1,O_k} + \sum_{i=0}^{i'}\sum_{j=0}^{j'} \triangle e^{WCL}_{p,k',h+1,i,j} + \sum_{i=0}^{i'}\sum_{j=0}^{j'} \triangle e_{p,k',h+1,i,j} \\ \geq -\left(\sum_{i=i'}^{N}\sum_{j=j'}^{N} \triangle e^{WCL}_{p,k',h+1,i,j} + \sum_{i=i'}^{N}\sum_{j=j'}^{N} \triangle e_{p,k',h+1,i,j}\right) \end{aligned} \tag{14B}$$

where $e_{p,k',h+1,O_k}$ is the SOC at the point when $p$ E-bus starts the next loop. The calculation of $\triangle e_{p,k',h+1,i,j}$ is shown by Equation (20) in Section 4.4, and the calculation of $\triangle e^{WCL}_{p,k',h+1,i,j}$ is shown by Equation (23) in Section 4.5.

**Constraint 3:** The length of a WCL on a road link should not be longer than the

link's length (i.e., dedicated bus lane's length) (as shown by Equation 15). This constraint is only applied in Scenario B.

$$0 \leq d_{i,j}^{WCL} \leq d_{i,j} \tag{15}$$

where $d_{i,j}$ is the length of $(i, j)$.

## 4.3 Simulation of E-bus's Possible Queuing at a Charging Station

In the E-bus operation, possible queuing at charging stations (because of limited charging posts) would directly affect the operational efficiency of the bus system, which needs to be considered in the selection and deployment of charging facilities.

To model the queueing system, we need a clear understanding of the major rules, including input process, queueing rules, and service rules, as shown in Table 2. For example, an E-bus will drive to a charging station for charging after it finishes the current loop. A charging station might have one or more charging posts, which could be either fast or slow (according to their power rates or charging speeds). A single queue of E-buses might be formed, waiting for the service of parallel charging posts. Each E-bus will consider whether to charge or leave without cutting in line, according to their schedule (or task), state of charge (SOC), (estimated) waiting time, etc.

Table 2 Major Rules of the Queueing System at a Charging Station

| Input process | Queueing rules | Service rules |
|---|---|---|
| The arrival time of each E-bus is dependent on its | ◆ Hybrid queueing rule: for those E-buses with sufficient electricity for their next task (i.e., loop), they will leave the queue if their waiting time is too | ◆ first-come, first-served (FCFS) |

| | | |
|---|---|---|
| own timetable. | long (we call it dropout here); while for those without sufficient electricity for the next task (i.e., loop), there would be no dropout.<br>◆ The queueing capacity is unlimited. | (Laguna & Marklund, 2019) |
| | ◆ Several parallel servers–single queue: E-buses line up, and there are several charging posts that can be either fast or slow. | |

Based on the queueing system's operating rules above, we need to further estimate each E-bus's timeline, which is essential for ensuring that they can complete their task on time. Fig. 5 shows the queueing timeline that an E-bus might experience when arriving at a charging station.

The time spent by an E-bus at a charging station ($t_{(m,k,p,h,sy)}$) is related to the latest time of the E-bus that needs to leave the station ($T_{(m,k,p,h,sp)}$) and the time of the E-bus that arrives at the station ($T_{(m,k,p,h,ar)}$), as described by Equation (16).

$$t_{(m,k,p,h,sy)} = T_{(m,k,p,h,sp)} - T_{(m,k,p,h,ar)} \tag{16}$$

The time spent by an E-bus that charges in a station ($t_{(m,k,p,h,pl)}$) is related to the time if the E-bus has charged until its battery is full or enough for the next loop ($T_{(m,k,p,h,fs)}$) and the time of the E-bus that starts charging ($T_{(m,k,p,h,st)}$), as described by Equation (17).

$$t_{(m,k,p,h,pl)} = T_{(m,k,p,h,fs)} - T_{(m,k,p,h,st)} \tag{17}$$

The delay time of an E-bus ($t_{(m,k,p,h,ps)}$) is related to the latest time of the E-bus that needs to leave the station ($T_{(m,k,p,h,sp)}$) and the time if the E-bus has charged until its battery is full or enough for the next loop ($T_{(m,k,p,h,fs)}$), as described by Equation

(18).

$$t_{(m,k,p,h,ps)} = T_{(m,k,p,h,sp)} - T_{(m,k,p,h,fs)} \tag{18}$$

The relationship between the time of an E-bus starts charging ($T_{(m,k,p,h,st)}$) and the time of a charging post that can provide charging service ($T_{m,x_{f\ or\ s,m},p',h_k,fs}$), can be mathematically described by Equation (19).

$$T_{(m,k,p,h,st)} = min\left\{T_{m,1,p',h_k,fs}, T_{m,2,p',h_k,fs}, \dots\dots, T_{m,x_{f\ or\ s,m},p',h_k,fs}\right\} \tag{19}$$

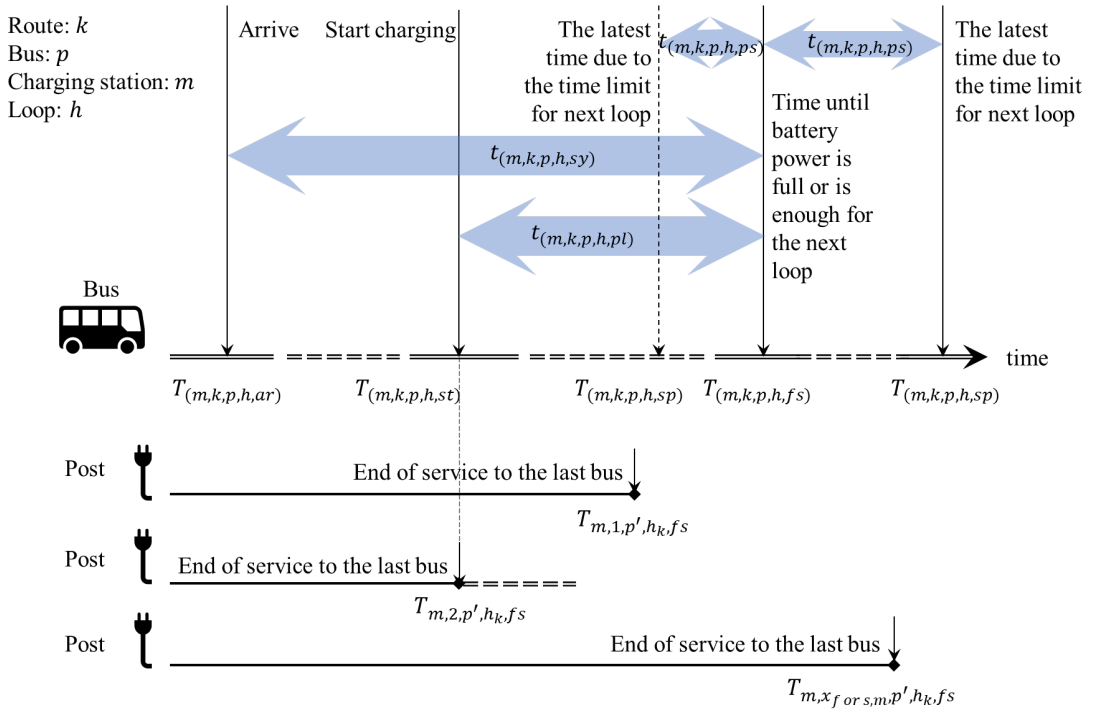


Fig. 5 Queueing Timeline of E-buses at a Charging Station

The hybrid queuing rules above can be implemented following the flowchart shown in Fig. 6. Several judgments (e.g., whether the E-bus has sufficient electricity for the next task, whether the E-bus is delayed, whether the E-bus can get service immediately, and whether the battery is full) are essential. They could affect the time spent by the E-

bus, which could be used to evaluate the service level of a charging station.

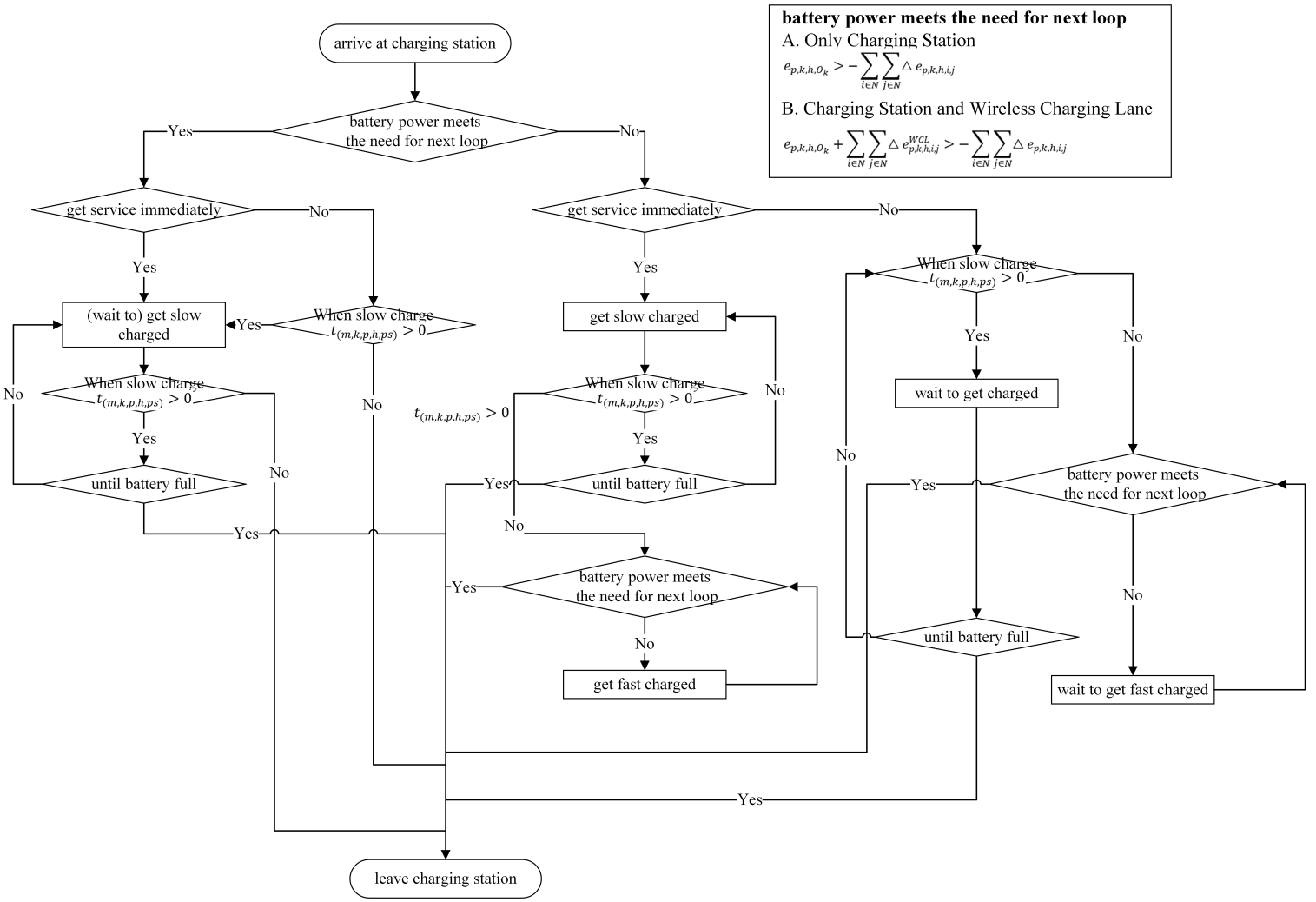


Fig. 6 Process of the Hybrid Queuing Rules

## 4.4 Simulation of E-bus's Electricity Consumption

In the simulation, we need to calculate electricity consumption and update the state of charge (SOC) for each E-bus when they are moving on the road network. This could help understand when and where E-buses need to get recharged (i.e., the spatial and temporal distributions of E-bus charging demand.

E-bus's energy consumption could be influenced by many factors (Basma, Mansour, Haddad, Nemer, & Stabat, 2022; Chen, Zhang, & Sun, 2021; Liu, Gao, Wang, Feng, & Li, 2022; Pamula & Pamula, 2020). Here, based on the investigation of the actual operation of buses, an estimate method supposed by Pamula and Pamula (2020) was used to calculate electricity consumption ($\triangle e_{p,k,h,i,j}$) in the simulation, considering several key influential factors, including travel distance ($d_{ij}$), travel duration ($t_{ij}$), elevation differences ($h_{ij}$), and environment ($w_{ij}$), as represented by Equation (20).

$$\triangle e_{p,k,h,i,j} = f\left(d_{ij}, t_{ij}, c_{ij}, w_{ij}\right) = m_4 d_{ij} + m_3 t_{ij} + m_2 h_{ij} + m_1 w_{ij} + b \qquad (20)$$

where $m_1, m_2, m_3, m_4, b$ are the parameters that affect the energy consumption of E-bus by weather, elevation, travel time and travel distance, respectively.

With the energy consumption model, we could update an E-bus's SOC after they pass a road link ($e_{p,k,h,j}$) using Equation (21).

$$e_{p,k,h,j} = e_{p,k,h,i} + \triangle e_{p,k,h,i,j} \qquad (21)$$

## 4.5 Simulation of E-bus's Charging Event

We proposed two methods to simulate charging events at a charging station (Case 1) and on WCLs (Case 2), respectively.

**Case 1: Charging at a charging station**

The amount of electricity that an E-bus can obtain through a charging post ($\triangle e_{p,k,h,m}$) is determined by its charging power ($a_f$ for fast charging post or $a_s$ for slow charging post), charging efficiency ($Eff_f^{Sta}$ for fast charging posts and $Eff_s^{Sta}$ for slow ones), and charging duration ($t_{p,k,h,m,f}$ for fast charging posts and $t_{p,k,h,m,s}$ for slow ones), as shown by Equation (22). It is worth noting that $t_{p,k,h,m,f} = 0$ if the E-bus uses a slow charging post and $t_{p,k,h,m,s} = 0$ if the E-bus use a fast one.

$$\triangle e_{p,k,h,m} = a_f \times t_{p,k,h,m,f} \times Eff_f^{Sta} + a_s \times t_{p,k,h,m,s} \times Eff_s^{Sta} \quad (22)$$

**Case 2: Charging through a wireless charging lane (WCL)**

Similarly, the amount of electricity that an E-bus can obtain through a WCL ($\triangle e_{p,k,h,i,j}^{WCL}$) is determined by the WCL's charging power ($a_{WCL}$), charging efficiency ($Eff^{WCL}$), and charging duration ($t_{i,j}^{WCL}$), as shown by Equation (23).

$$\triangle e_{p,k,h,i,j}^{WCL} = t_{i,j}^{WCL} \times a_{WCL} \times Eff^{WCL} \quad (23)$$

We assume that the E-buses travel at a constant speed on each link (as analyzed in Section 3.2), since most of the road links in the network are quite short, with an average

length of 17.5 meters. Therefore, if the E-bus has not been fully charged after traveling on this WCL, the charging duration ($t_{i,j}^{WCL}$) is equal to the E-bus's travel time on the WCL ($t_{i,j}^{WCL}$), which can be represented by the ratio of lengths of the wireless charging lane ($d_{i,j}^{WCL}$) to the road ($d_{i,j}$) and the average travel time on the road ($t_{i,j}$). If the E-bus has been fully charged on the WCL, the charging duration ($t_{i,j}^{WCL}$) is also related to its battery capacity ($c_p$), the SOC before the WCL ($e_{p,k,h,i}$) and electricity consumption ($\triangle e_{p,k,h,i,j}$). Equation (24) shows the calculation of charging duration ($t_{i,j}^{WCL}$).

$$t_{i,j}^{WCL} = \begin{cases} \dfrac{d_{i,j}^{WCL} \times t_{i,j}}{d_{i,j}}, if\ the\ battery\ is\ not\ fully\ charged \\ \dfrac{c_p - e_{p,k,h,i} + \triangle e_{p,k,h,i,j}}{a_{WCL} \times Eff^{WCL}}, if\ the\ battery\ is\ fully\ charged \end{cases} \quad (24)$$

## 4.6 Decision Variables and Algorithms

A set of decision variables can be adjusted in searching for optimal solutions in the model. These variables are related to charging facilities, including the number and location of charging stations ($M$), the number and allocation of charging posts ($X_{f,m}$ and $X_{s,m}$), battery capacity of an E-bus ($c_p$), and the length and location of a WCL ($d_{i,j}^{WCL}$) (only for Scenario B). The information on how we set the model parameters with the sources provided can be found in Table C.3 in Appendix C.

This study used the back propagation neural network-genetic algorithm (BP-GA) and non-dominated sorting genetic algorithms-II (NSGA-II) (Deb, Pratap, Agarwal, & Meyarivan, 2002) to solve the optimization model. This combines the better

adaptability of GA to the optimization problem with the adaptive learning ability of BP to obtain a more efficient problem-solving ability (Jin et al., 2021). Specifically, the task of GA is to discover good solutions in the solution space, and the task of BP is to assess the NSGA-II fitness value of the solution that GA offers. The Pareto optimal set of the bi-objective optimization model will be output when the process meets the end criterion (i.e., either the number of iterations or NSGA-II fitness value reaches a maximum). Fig. 7 shows the flow chart of BP-GA and NSGA-II. The key parameters were set through trial and error: crossover probability was set to 0.9, mutation probability was set to 0.1, population size was set to 50, and the network was comprised of three layers of units (nodal points).

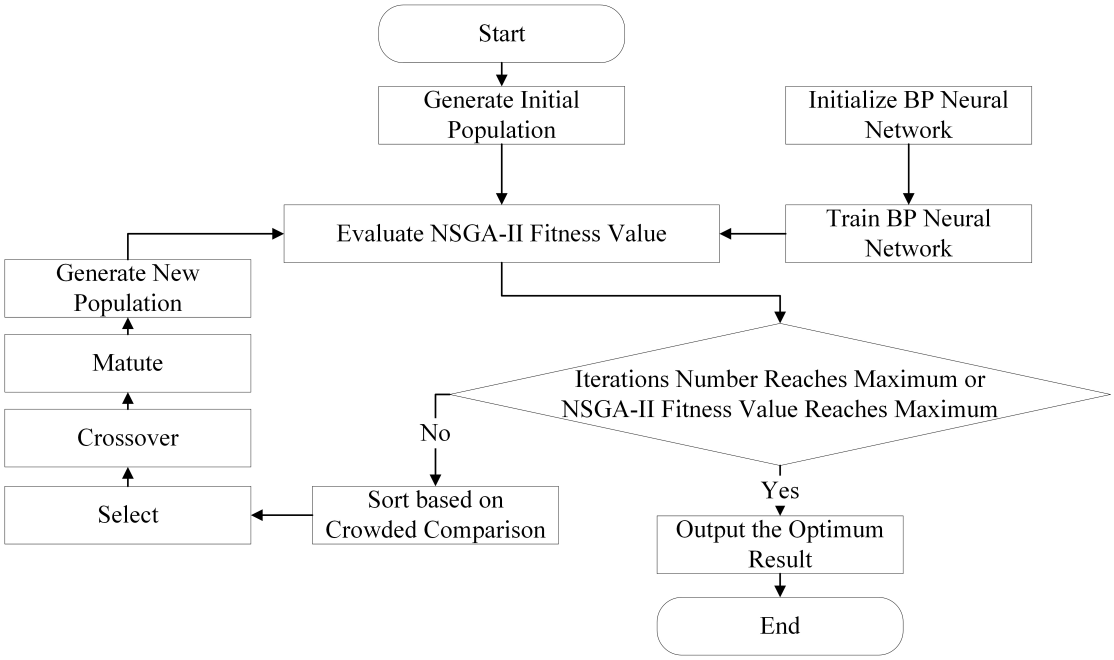


Fig. 7 Flow Chart of BP-GA (Source: Adapted from Huang, Han, Wan, Ma, and Chen (2016); Li, Wang, Xu, Ni, and Sun (2022)).

# 5 Case Study of New York City

## 5.1 Results

### 5.1.1 Deployment of Charging Facilities

We got two sets of optimal solutions for the two scenarios (Scenarios A and B), respectively, and each set has 49 solutions, as shown in Fig. 8. Each solution in the set is optimal. The E-bus company could make a trade-off between total cost and total delay time and choose the solution which can better meet their needs.

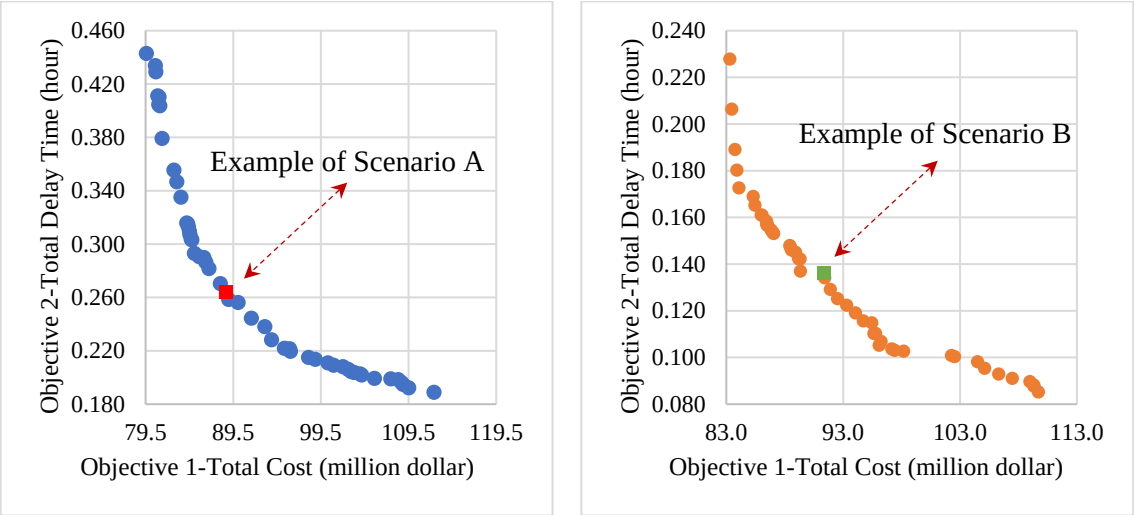


(a) Scenario A (b) Scenario B

Fig. 8 Pareto Optimal Solutions for Bi-objective Optimization Models in Scenarios A and B

To compare the suitability of traditional charging posts and WCLs in the electrified bus network, we first sorted all the solutions in the optimal solution set by the total cost (smallest to largest) and then chose the median solution for both Scenarios A and B. Such a comparison method has been widely used in those studies involving Pareto

optimal solutions (Farmani, Savic, & Walters, 2005; Kahloul, Zouache, Brahmi, & Got, 2022; Ryu & Baik, 2016), Fig. 9 shows the key difference between Scenarios A and B in objective values and design variables.

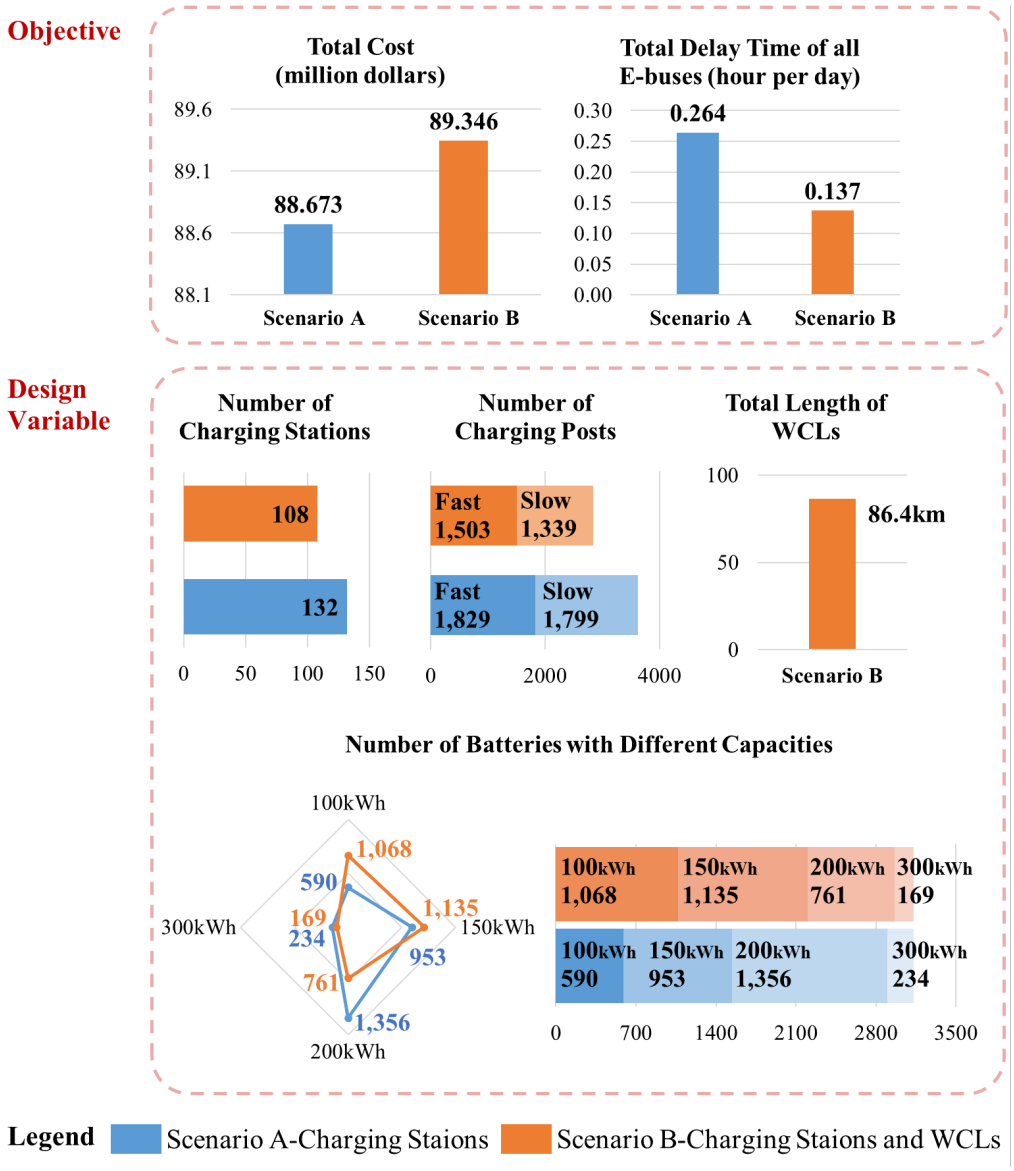


Fig. 9 Selected Pareto Optimal Solutions including Design Variables and Objective Values in Scenarios A and B

For Scenario A with only charging stations available, 132 charging stations with 1,829 fast charging posts and 1,799 slow ones are needed for the whole E-bus system. Fig. 10 shows the spatial distribution of these charging facilities. In addition, the

numbers of E-bus batteries with capacities of 100 kWh, 150 kWh, 200 kWh, and 300 kWh are 590, 953, 1356, and 234, respectively. The whole E-bus system costs 88.673 million dollars with a total delay time of 0.264 hours per day of all E-buses.

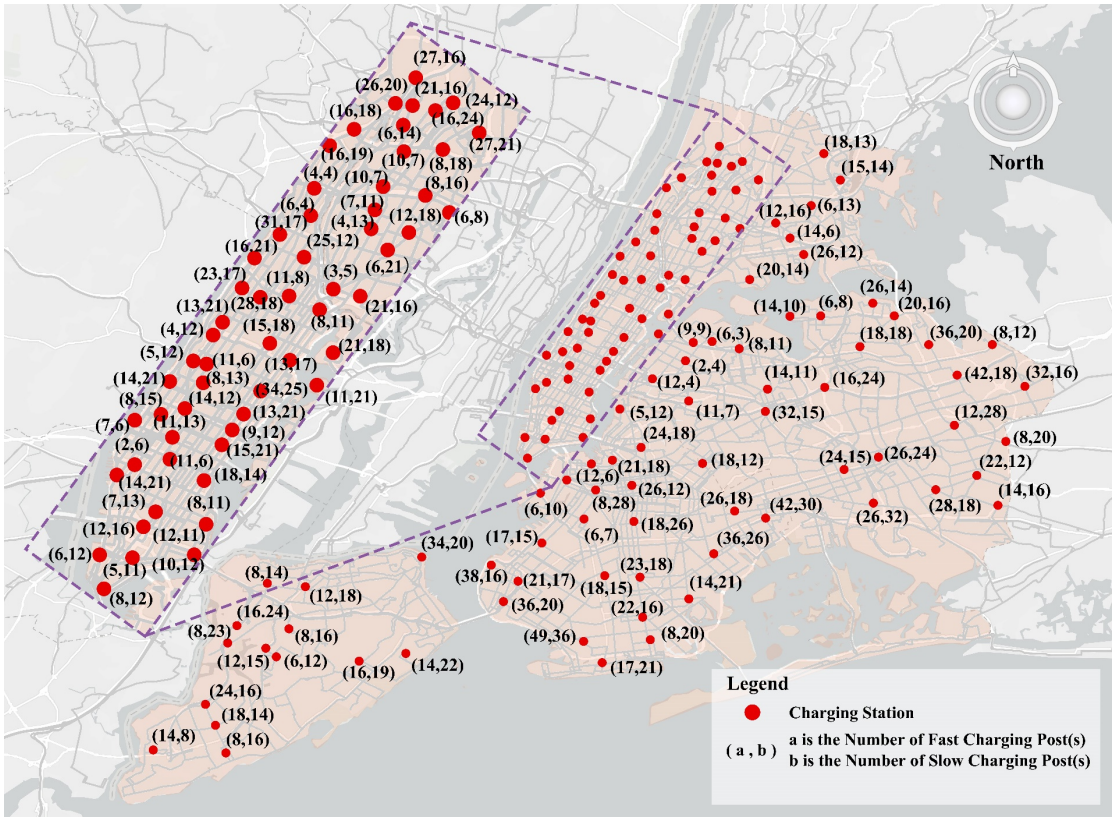


Fig. 10 The Layout of Charging Stations and Charging Posts in Scenario A

For Scenario B with both charging stations and wireless charging lanes (WCLs) available, 108 charging stations with 1,503 fast charging posts and 1,339 slow ones, and 86.4 km WCLs are needed in the whole E-bus system. Fig. 11 shows the layout of charging facilities. In addition, the numbers of E-bus batteries with capacities of 100 kWh, 150 kWh, 200 kWh, and 300 kWh are 1068, 1135, 761, and 169, respectively. The E-bus system costs 89.346 million dollars in total, with a total delay time of 0.137 hours per day for all E-buses.

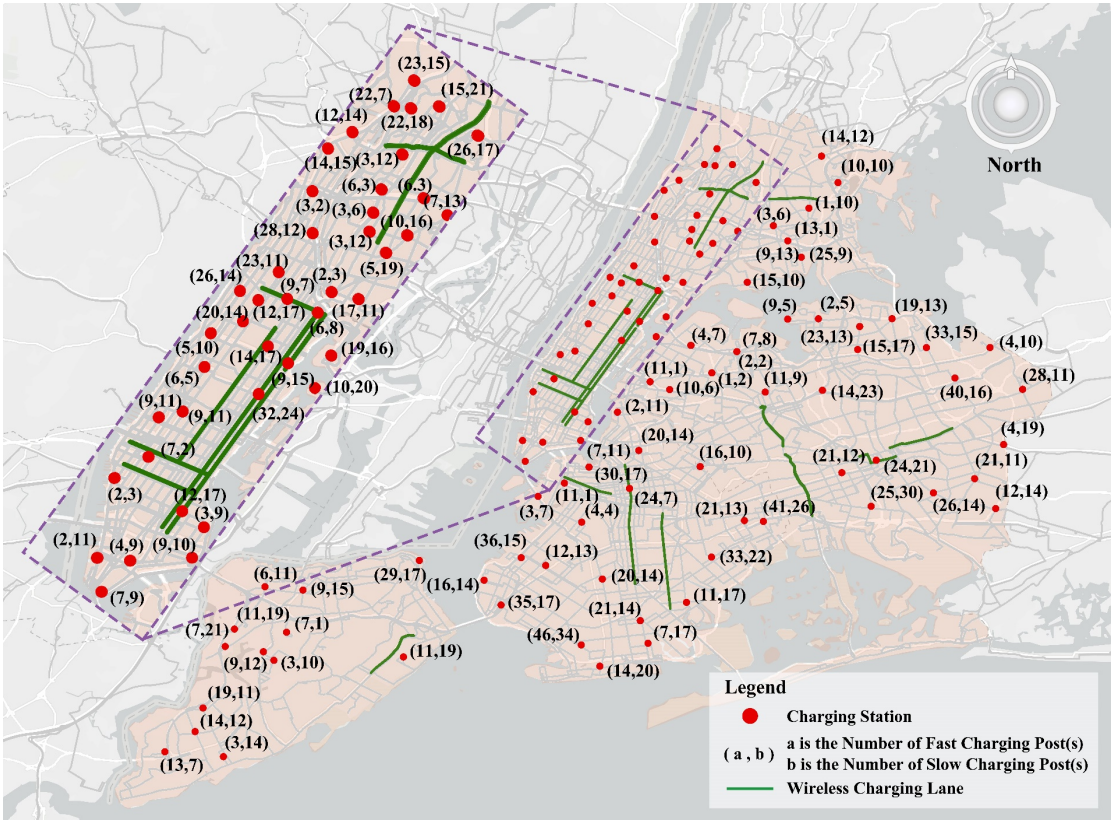


Fig. 11 The Layout of Charging Stations and Charging Posts and WCLs in Scenario B

For design variables, Scenario A got more stations and charging posts than Scenario B to accommodate the charging demand, as Scenario B got a few WCLs. To ensure efficiency, Scenario A needs more fast charging posts. The battery capacities of Scenarios A and B vary greatly: more high-capacity batteries are needed in Scenario A, likely because the E-buses can only get charged at charging stations when they finish one loop, and thus the capacity should be high enough to store sufficient electricity. While in Scenario B (with both charging stations and WCLs available), the E-bus batteries can get recharged on their journeys, and thus, capacity does not have to be too high.

For objective values, the numbers of charging stations, charging posts, and high-

capacity batteries are smaller in Scenario B, but the cost of WCLs is quite high. As a result, the total cost of Scenario B is 0.76% higher than that of Scenario A. However, a bit higher cost in Scenario B could give rise to a substantial improvement in the level of service, as evident from the much shorter delay time in Scenario B (Specifically, the total delay time in Scenario B is 48.11% shorter than that in Scenario A).

### 5.1.2 Quantification of Energy and Environmental Benefits

In order to evaluate the environmental benefit, we used Life Cycle Analysis (LCA) method to compare the production, use, and end-of-life stages of vehicles and charging facilities in the baseline scenario, Scenarios A and B. Specifically, GREET 2022 was adopted to assess the energy consumption and carbon emissions on cradle-to-grave (C2G) stages (ANL (Argonne National Laboratory), 2022) , as it has been widely used in many transport studies for LCA (Wong, Ho, So, Tsang, & Chan, 2021; Yang et al., 2021; Yu, Cong, Hui, Zhao, & Yu, 2022). For vehicles (buses), the fuel-cycle, including well-to-pump (WTP) and pump-to-wheel (PTW) stages, was evaluated by the GREET1 Model (a sub-model of GREET 2022 for fuel-cycle); the vehicle-cycle, including vehicle manufacturing cycle (VMC) (including battery manufacturing cycle) and vehicle end of life (EOL) stages, was evaluated by the GREET2 Model (a sub-model of GREET 2022 for vehicle-cycle). For charging stations and WCLs, the C2G stages were based on the GREET Building LCA Module (a sub-model of GREET 2022 for building). More detailed information on LCA can be found in Appendix D.

Table 3 shows the evaluation results of energy consumption and carbon emissions in the baseline scenario (where conventional vehicles are used in the bus fleet), Scenarios A (with E-buses and charging stations) and B (with E-buses, charging stations and WCLs). The C2G stages in Scenarios A and B have good energy saving and emission reduction benefits, with energy consumption reduced by 64.76% and 68.33%, and carbon emissions reduced by 68.78% and 71.93%, respectively, compared to the baseline scenario. Scenario B has a better performance than Scenario A, since WCLs allow E-buses to use a smaller battery size, which can help to greatly reduce the weight of the battery and thus save energy and reduce emissions, though WCLs also consume resources and emit emissions.

Table 3 Energy Consumptions and Emissions in the Baseline Scenario, Scenario A and Scenario B

| **Scenario** | **Energy Consumption (tj/year)** | | | | **Emissions (including VOC, CO, CO2) (ton/year)** | | | |
|---|---|---|---|---|---|---|---|---|
| | Vehicle | Charging Station | WCL | **Total** | Vehicle | Charging Station | WCL | **Total** |
| Baseline Scenario | 1070.820 | N.A. | N.A. | 1070 | 71358.956 | N.A. | N.A. | 71359 |
| Scenario A | 377.298 | 0.015 | N.A. | 377 | 22274.362 | 2.868 | N.A. | 22277 |
| Scenario B | 339.111 | 0.013 | 0.006 | 339 | 20026.475 | 2.346 | 0.985 | 20030 |

Note: To be consistent with Section 5.1.1, we used the median solutions in Scenarios A and B for comparison.

## 5.2 Parameter Sensitivity Analysis

Parameter values may significantly influence the model outputs of interest. Therefore, we conducted a sensitivity analysis to test how four important parameters, namely,

vehicle cost (without battery cost) (per-unit) (\$/vehicle) $C^{veh}$, battery cost (per-unit) (\$/kWh) $C^{bat,m}$, charging power of wireless charging lane (kW) $a_{WCL}$, charging efficiency of wireless charging lane (%) $Eff^{WCL}$, would influence the two objective values, i.e., Objective 1 - total cost, and Objective 2 - total delay time. Specifically, these four parameters varied between -50% ~ +50%, with an interval of 10% in both Scenarios A and B. Fig. 12 shows the sensitivity analysis results.

For the two cost-related parameters, vehicle cost (without battery cost) (per-unit) (\$/vehicle) ($C^{veh}$) and battery cost (per-unit) (\$/kWh) ($C^{bat,m}$), their rise would give increases in both Objective 1 and Objective 2, namely total cost and total delay time, in both Scenarios A and B. For instance, when $C^{veh}$ is increased by 50% (see Fig. 12-(a)), the total cost in Scenario A is increased by 24.20%, and the total delay time is increased by 28.32%; while in scenario B, the total cost is increased by 15.12%, and the total delay time is increased by 26.70%. For $C^{bat,m}$, when it is increased by 50% (see Fig. 12-(b)), the total cost in Scenario A is increased by 14.61%, and the total delay time is increased by 33.85%; while in Scenario B, the total cost is increased by 13.17%, and the total delay time is increased by 24.54%. To sum up, it could be seen that the increase in these two parameters (i.e., vehicle cost (without battery cost) and battery cost) might have a more significant impact in Scenario A, which both influence the total vehicle cost. In searching for optimal solutions, the model will make a trade-off between Objective Functions 1 and 2, which could influence the contribution of items in the objective functions to the function values (Miettinen, 1999). Therefore, an increase in

the vehicle cost (without battery cost) may influence the other cost types in Objective Function 1, and further the associated design variables. For example, due to a significant increase in the vehicle cost (without battery cost), the battery cost could be decreased, and further the vehicle's battery capacity (which is a design variable) is decreased. This might lead to the E-buses needing to be charged more times (i.e., a higher charging frequency) to perform the same transport tasks, making up for the reduction in the amount of electricity it carries (i.e., battery capacity). In Scenario A, only charging stations provide charging services, and the optimization operation has no choice but to accept the increased cost of charging stations and posts to meet the charging demand. As for Scenario 2, WCLs with an efficient charging mode could also provide charging services, and the system might transfer more charging demand to WCLs. In addition, according to the analysis in Section 5.1, Scenario A might require higher battery capacities than Scenario B. Thus, Scenario A needs to pay more for batteries to maintain its service level.

For the two key parameters related to WCLs, charging power of wireless charging lane (kW) ($a_{WCL}$), charging efficiency of wireless charging lane (%) ($Eff^{WCL}$), when they are increased in Scenario B, both Objective 1 and Objective 2 might decrease. For example, for $a_{WCL}$, when it is increased by 50%, the total cost is decreased by 23.65%, and the total delay time is reduced by 47.16%, as shown in Fig. 12-(c). For $Eff^{WCL}$, when it is increased by 50%, the total cost is decreased by 39.86%, and the total delay time is reduced by 39.47%, as shown in Fig. 12-(d). This might be because the increases

in both charging power and charging efficiency of WCL would allow E-buses to obtain more electricity within the same charging duration. This could further reduce the demand for charging stations/posts and further the total cost. Also, this could reduce charging demand at charging posts, which can lead to a shorter delay time.

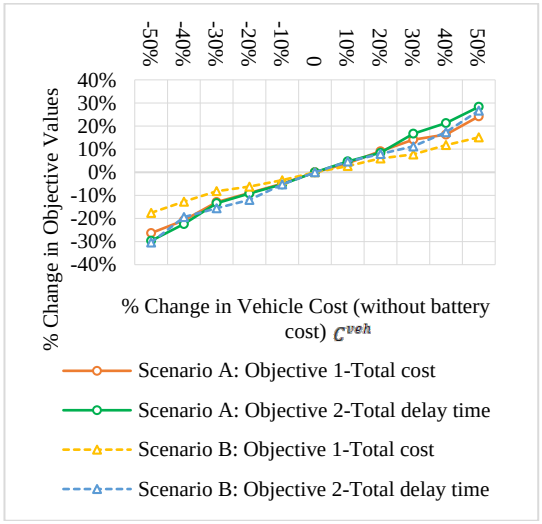


(a) Vehicle Cost (without battery cost) (per-unit) ($/vehicle) ($C^{veh}$)

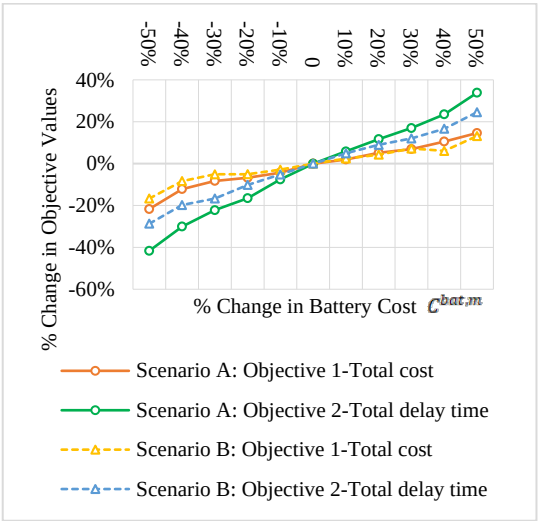


(b) Battery Cost (per-unit) ($C^{bat,m}$)

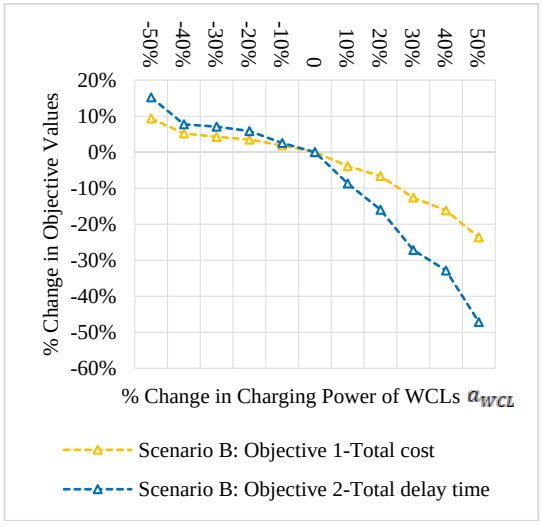


(c) Charging Power of WCLs ($a_{WCL}$) (only applicable to Scenario B)

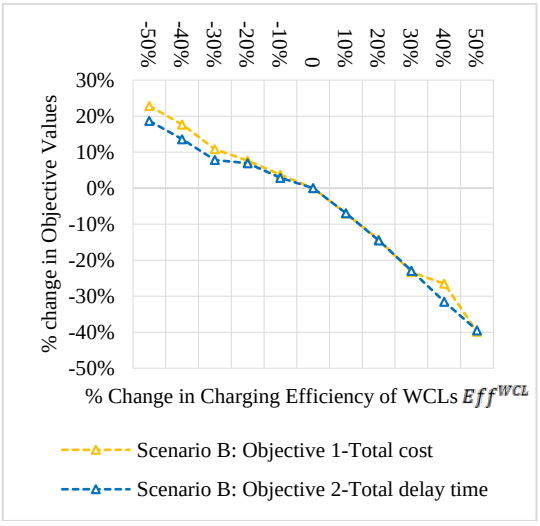


(d) Charging Efficiency of WCLs ($Eff^{WCL}$) (only applicable to Scenario B)

Fig. 12 Results of Sensitivity Analysis: Influences on the two Objective Values

Note: For the y-axis: in terms of Objective 1 in Scenarios A and B, we used the values of Objective 1-Total cost (i.e., 88.673 and 89.346 million dollars, respectively) as references, in terms of Objective 2 in Scenarios A and B, we used the values of

Objective 2-Total delay time (i.e., 0.264 and 0.137 hours per day, respectively) as references, and then we converted the objective values from all tests into percentages.

# 6 Conclusion

This study developed a data-driven micro-simulation-based bi-objective optimization models to deploy charging facilities for large-scale bus networks. In particular, we compared performance of traditional charging posts and wireless charging lanes (WCLs). The results indicated that the scenario with both charging posts and WCLs deployed has a slightly higher cost (i.e., 0.76% higher) than the scenario with only charging posts deployed. However, the former scenario has a much higher level of service with 48.11% shorter total delay time. This indicates that WCLs present a promising charging approach which can greatly improve the level of service (but has a slightly higher cost). The results of LCA show that Scenarios A and B both have significant environmental benefits, with energy consumption reduced by 64.76% and 68.33%, and carbon emissions reduced by 68.78% and 71.93% from the baseline scenario, respectively. In addition, the parameter sensitivity analysis results indicated that the parameters related to vehicles and facilities, i.e., vehicle cost (without battery cost) (per-unit) ($/vehicle), battery cost (per-unit) ($/kWh), charging power of wireless charging lane (kW), and charging efficiency of wireless charging lane (%), were influential to the model outputs of interest, i.e., the total cost and the total delay time.

The above results show that bus system electrification can contribute to energy conservation and environmental protection while ensuring the fulfilment of transport

tasks. Moreover, the scenario with both charging stations and WCLs deployed has a higher level of service and higher environmental benefits than the scenario with only charging stations deployed, though it also requires a higher cost. Our study can provide bus operators with useful information for them to choose between different kinds of charging facilities, as well as optimal charging facility deployment and fleet battery configuration solutions. In addition, the Life Cycle Analysis (LCA) results can help the transit operator understand how much energy can be saved and carbon emission can be reduced, and further the extent to which the optimal solutions can contribute to the Net-zero commitments and Sustainable Development Goals (SDGs).

The optimization model can be further improved in future work. First, one-day real bus GPS trajectory data have been used to develop the data-driven micro-simulation model. The model could be improved by using a larger dataset with more bus trajectories collected over a longer period. For example, a one-week dataset would allow us to consider the differences between weekdays and weekends in the bus operation; a one-year dataset would allow us to take seasonal effects into account additionally. Second, one limitation of the proposed data-driven micro-simulation approach is that the timetable of E-buses was assumed to be constant (i.e., consistent with the real world). However, cost reduction could be achieved by optimizing the fleet size and a feasible assignment of E-bus trips. Therefore, since the proposed approach is a bi-objective optimization processing, which could be extended as a multi-objective optimization approach to optimize the E-bus operation jointly. Third, the land use and

labour supply might influence the cost of facility construction, and thus could be considered in the optimization model. This is expected to obtain more realistic model outputs.

## Acknowledgement

The work described in this paper was jointly supported by the National Natural Science Foundation of China (52002345), the research grants from the Research Institute for Sustainable Urban Development (1-BBWF and 1-BBWR), the Smart Cities Research Institute (CDAR and CDA9) and the funding for Project of Strategic Importance provided by The Hong Kong Polytechnic University (1-ZE0A).

## References

Abdelwahed, A., van den Berg, P. L., Brandt, T., Collins, J., & Ketter, W. (2020). Evaluating and optimizing opportunity fast-charging schedules in transit battery electric bus networks. Transportation Science, 54(6), 1601-1615. doi:10.1287/trsc.2020.0982

Alwesabi, Y., Liu, Z., Kwon, S., & Wang, Y. (2021). A novel integration of scheduling and dynamic wireless charging planning models of battery electric buses. Energy (Oxford), 230, 120806. doi:10.1016/j.energy.2021.120806

Alwesabi, Y., Wang, Y., Avalos, R., & Liu, Z. (2020). Electric bus scheduling under single depot dynamic wireless charging infrastructure planning. Energy (Oxford), 213, 118855. doi:10.1016/j.energy.2020.118855

Andrew Catania, L. K., Eugene Tseng, Michael Woods. (2019). Every city: Accelerating electric bus adoption in the New York City MTA bus system. New York City, United States: School of International and Public Affairs, Columbia University.

ANL (Argonne National Laboratory). (2022, November 7). GREET model. Retrieved from https://greet.es.anl.gov/

Authority, N. Y. P. (2021, May 27). NYPA supports electrification of NYC buses with $39M overhead electric bus charger infrastructure project. Retrieved from

https://electricenergyonline.com/article/energy/category/ev-storage/143/901349/nypa-supports-electrification-of-nyc-buses-with-39m-overhead-electric-bus-charger-infrastructure-project.html

Basma, H., Mansour, C., Haddad, M., Nemer, M., & Stabat, P. (2022). Energy consumption and battery sizing for different types of electric bus service. Energy (Oxford), 239, 122454. doi:10.1016/j.energy.2021.122454

Buja, G., Bertoluzzo, M., & Dashora, H. K. (2016). Lumped track layout design for dynamic wireless charging of electric vehicles. IEEE Transactions on Industrial Electronics, 63(10), 6631-6640. doi:10.1109/Tie.2016.2538738

Chen, J., Atasoy, B., Robenek, T., Bierlaire, M., & Thémans, M. (2013). Planning of feeding station installment for electric urban public mass-transportation system. Paper presented at the 13th Swiss Transportation Research Conference, Ascona, Switzerland.

Chen, Y., Zhang, Y., & Sun, R. (2021). Data-driven estimation of energy consumption for electric bus under real-world driving conditions. Transportation Research. Part D, Transport and Environment, 98(C), 102969. doi:10.1016/j.trd.2021.102969

Chen, Z., Yin, Y., & Song, Z. (2018). A cost-competitiveness analysis of charging infrastructure for electric bus operations. Transportation Research. Part C, Emerging Technologies, 93, 351-366. doi:10.1016/j.trc.2018.06.006

Deb, K., Pratap, A., Agarwal, S., & Meyarivan, T. (2002). A fast and elitist multiobjective genetic algorithm: NSGA-II. IEEE Transactions on Evolutionary Computation, 6(2), 182-197. doi:10.1109/4235.996017

Eda, K., Kobayashi, M., Yang, W., Hirota, T., Kamiya, Y., & Daisho, Y. (2016). Performance evaluation of short range frequent charging Electric Bus (third report): Reduction of CO2 emissions in the long-term field test and possibility of further reduction of energy consumption. Jidōsha Gijutsukai Ronbunshū, 47(2), 401-406. doi:10.11351/jsaeronbun.47.401

Farmani, R., Savic, D. A., & Walters, G. A. (2005). Evolutionary multi-objective optimization in water distribution network design. Engineering Optimization, 37(2), 167-183. doi:10.1080/03052150512331303436

He, J., Yang, H., Tang, T.-Q., & Huang, H.-J. (2020). Optimal deployment of wireless charging lanes considering their adverse effect on road capacity. Transportation Research. Part C, Emerging Technologies, 111, 171-184. doi:10.1016/j.trc.2019.12.012

He, Y., Liu, Z., & Song, Z. (2020). Optimal charging scheduling and management for a fast-charging battery electric bus system. Transportation Research. Part E, Logistics and Transportation Review, 142(C), 102056. doi:10.1016/j.tre.2020.102056

He, Y., Liu, Z., & Song, Z. (2022). Integrated charging infrastructure planning and charging scheduling for battery electric bus systems. Transportation Research. Part D, Transport and Environment, 111. doi:10.1016/j.trd.2022.103437

He, Y., Song, Z., & Liu, Z. (2019). Fast-charging station deployment for battery electric

bus systems considering electricity demand charges. Sustainable Cities and Society, 48(C), 101530. doi:10.1016/j.scs.2019.101530

Hsu, Y.-T., Yan, S., & Huang, P. (2021). The depot and charging facility location problem for electrifying urban bus services. Transportation Research. Part D, Transport and Environment, 100, 103053. doi:10.1016/j.trd.2021.103053

Huang, M., Han, W., Wan, J., Ma, Y., & Chen, X. (2016). Multi-objective optimisation for design and operation of anaerobic digestion using GA-ANN and NSGA-II. Journal of Chemical Technology and Biotechnology (1986), 91(1), 226-233. doi:10.1002/jctb.4568

Hwang, I., Jang, Y. J., Ko, Y. D., & Lee, M. S. (2018). System optimization for dynamic wireless charging electric vehicles operating in a multiple-route environment. IEEE Transactions on Intelligent Transportation Systems, 19(6), 1709-1726. doi:10.1109/TITS.2017.2731787

IEA. (2022, November 25). Improving the sustainability of passenger and freight transport. Retrieved from https://www.iea.org/topics/transport

Iliopoulou, C., & Kepaptsoglou, K. (2019). Integrated transit route network design and infrastructure planning for on-line electric vehicles. Transportation Research. Part D, Transport and Environment, 77, 178-197. doi:10.1016/j.trd.2019.10.016

Jaiprakash, Habib, G., Kumar, A., Sharma, A., & Haider, M. (2017). On-road emissions of CO, CO2 and NOx from four wheeler and emission estimates for Delhi. Journal of Environmental Sciences (China), 53(3), 39-47. doi:10.1016/j.jes.2016.01.034

Jang, Y. J., Suh, E. S., & Kim, J. W. (2016). System architecture and mathematical models of electric transit bus system utilizing wireless power transfer technology. IEEE Systems Journal, 10(2), 495-506. doi:10.1109/JSYST.2014.2369485

Jin, Y., Li, Z., Han, Y., Li, X., Li, P., Li, G., & Wang, H. (2021). A research on line loss calculation based on BP neural network with genetic algorithm optimization. IOP Conference Series: Earth and Environmental Science, 675(1), 12155. doi:10.1088/1755-1315/675/1/012155

Kahloul, S., Zouache, D., Brahmi, B., & Got, A. (2022). A multi-external archive-guided Henry Gas Solubility Optimization algorithm for solving multi-objective optimization problems. Engineering Applications of Artificial Intelligence, 109, 104588. doi:10.1016/j.engappai.2021.104588

Kessler, E. (2022, April 22). MTA to add 60 Electric Buses by year’s end (that’s 1% of the entire fleet). Retrieved from https://nyc.streetsblog.org/2022/04/22/mta-to-add-60-electric-buses-by-years-end/

Laguna, M., & Marklund, J. (2019). Business process modeling, simulation and design (Third edition. ed.). Boca Raton, FL: CRC Press.

Lee, J., Shon, H., Papakonstantinou, I., & Son, S. (2021). Optimal fleet, battery, and charging infrastructure planning for reliable electric bus operations. Transportation Research. Part D, Transport and Environment, 100, 103066. doi:10.1016/j.trd.2021.103066

Li, M., Wang, G., Xu, J., Ni, J., & Sun, E. (2022). Life cycle assessment analysis and comparison of 1000 MW S-CO2 coal fired power plant and 1000 MW USC water-steam coal-fired power plant. Journal of Thermal Science, 31(2), 463-484. doi:10.1007/s11630-020-1327-x

Liu, H., Zou, Y., Chen, Y., & Long, J. (2021). Optimal locations and electricity prices for dynamic wireless charging links of electric vehicles for sustainable transportation. Transportation Research. Part E, Logistics and Transportation Review, 152, 102187. doi:10.1016/j.tre.2020.102187

Liu, K., Gao, H., Wang, Y., Feng, T., & Li, C. (2022). Robust charging strategies for electric bus fleets under energy consumption uncertainty. Transportation Research. Part D, Transport and Environment, 104, 103215. doi:10.1016/j.trd.2022.103215

Liu, X., Qu, X., & Ma, X. (2021). Optimizing electric bus charging infrastructure considering power matching and seasonality. Transportation Research. Part D, Transport and Environment, 100, 103057. doi:10.1016/j.trd.2021.103057

Liu, Z., & Song, Z. (2017). Robust planning of dynamic wireless charging infrastructure for battery electric buses. Transportation Research. Part C, Emerging Technologies, 83(C), 77-103. doi:10.1016/j.trc.2017.07.013

Machura, P., & Li, Q. (2019). A critical review on wireless charging for electric vehicles. Renewable & Sustainable Energy Reviews, 104, 209-234. doi:10.1016/j.rser.2019.01.027

Metropolitan Transportation Authority Bus Company. (2021, May 25). MTA announces plans to increase number of electric buses purchased in 2021. Retrieved from https://new.mta.info/press-release/mta-announces-plans-increase-number-of-electric-buses-purchased-2021

Meyer, R. (2014). Event-driven multi-agent simulation. Paper presented at the International Workshop on Multi-Agent Systems and Agent-Based Simulation, Cham.

Michael, S. (2017, December 1). New york city bus data. Retrieved from https://www.kaggle.com/datasets/stoney71/new-york-city-transport-statistics?select=mta_1712.csv

Miettinen, K. (1999). Nonlinear multiobjective optimization. Boston: Kluwer Academic Publishers.

Mouhrim, N., Alaoui, A. E. H., & Boukachour, J. (2016). Optimal allocation of wireless power transfer system for electric vehicles in a multipath environment. Paper presented at the 2016 3rd International Conference on Logistics Operations Management (GOL).

Ngo, H., Kumar, A., & Mishra, S. (2020). Optimal positioning of dynamic wireless charging infrastructure in a road network for battery electric vehicles. Transportation Research. Part D, Transport and Environment, 85, 102385. doi:10.1016/j.trd.2020.102385

NYC Department of Transportation. (2021, September 20). Electrifying New York: An electric vehicle vision plan for New York City. Retrieved from

https://www1.nyc.gov/html/dot/downloads/pdf/electrifying-new-york-report.pdf

NYCOpenData. (2021, February 3). Bus lanes - local streets. Retrieved from https://data.cityofnewyork.us/Transportation/Bus-Lanes-Local-Streets/ycrg-ses3

OpenStreetMap. (2021, April 4). OpenStreetMap data. Retrieved from http://download.geofabrik.de/north-america/us/new-york.html

Pamula, T., & Pamula, W. (2020). Estimation of the energy consumption of battery electric buses for public transport networks using real-world data and deep learning. Energies (Basel), 13(9), 2340. doi:10.3390/en13092340

Port Auyhority NYNJ. (2008, November 17). Architect chosen for planned office tower above port authority bus terminal's north wing. Retrieved from https://www.panynj.gov/port-authority/en/press-room/press-release-archives/2008_press_releases/architect_chosenforplannedofficetowerabovepor tauthoritybustermin.html

Rogge, M., van der Hurk, E., Larsen, A., & Sauer, D. U. (2018). Electric bus fleet size and mix problem with optimization of charging infrastructure. Applied Energy, 211, 282-295. doi:10.1016/j.apenergy.2017.11.051

Ryu, D., & Baik, J. (2016). Effective multi-objective naïve Bayes learning for cross-project defect prediction. Applied Soft Computing, 49, 1062-1077. doi:10.1016/j.asoc.2016.04.009

Swedish Electromobility Centre. (2019, March 3). Power conversion challenges with an all-electric land transport system. Retrieved from http://emobilitycentre.se/wp-content/uploads/2019/09/Power-Conversion-Challenges-with-an-All-Electric-Land-Transport-System.pdf

Topal, O., & Nakir, İ. (2018). Total cost of ownership based economic analysis of diesel, CNG and electric bus concepts for the public transport in Istanbul City. Energies (Basel), 11(9), 2369. doi:10.3390/en11092369

United Nations. (2022). The sustainable development goals report 2022. Retrieved from https://unstats.un.org/sdgs/report/2022/The-Sustainable-Development-Goals-Report-2022.pdf

United Nations Environment Programme. (2022). Emissions gap report 2022. Retrieved from https://www.unep.org/resources/emissions-gap-report-2022?gclid=Cj0KCQiAyracBhDoARIsACGFcS5Mr5bdLHBm6R6MOew8vTlXub-vN0wxGC2KNmb6YY6XNCdr0aW-Us0aApP6EALw_wcB

Ushijima-Mwesigwa, H., Khan, M. D. Z., Chowdhury, M. A., & Safro, I. (2017). Optimal installation for electric vehicle wireless charging lanes. arXiv preprint. doi:10.48550/arxiv.1704.01022

Uslu, T., & Kaya, O. (2021). Location and capacity decisions for electric bus charging stations considering waiting times. Transportation Research. Part D, Transport and Environment, 90, 102645. doi:10.1016/j.trd.2020.102645

Wang, Q. C., Sigler, D., Liu, Z. C., Kotz, A., Kelly, K., & Phillips, C. (2022). Aspires: Airport shuttle planning and improved routing event-driven simulation.

Transportation Research Record. doi:10.1177/03611981221095744

Wang, T., Yang, B., Chen, C., & Guan, X. (2019, 28 April - 01 May). Wireless charging lane deployment in urban areas considering traffic light and regional energy supply-demand balance. Paper presented at the 2019 IEEE 89th Vehicular Technology Conference (VTC2019-Spring).

Wang, Y., Liao, F., & Lu, C. (2022). Integrated optimization of charger deployment and fleet scheduling for battery electric buses. Transportation Research. Part D, Transport and Environment, 109. doi:10.1016/j.trd.2022.103382

Wong, E. Y. C., Ho, D. C. K., So, S., Tsang, C. W., & Chan, E. M. H. (2021). Life cycle assessment of electric vehicles and hydrogen fuel cell vehicles using the GREET model-A comparative study. Sustainability, 13(9). doi:10.3390/su13094872

Wu, X., Feng, Q., Bai, C., Lai, C. S., Jia, Y., & Lai, L. L. (2021). A novel fast-charging stations locational planning model for electric bus transit system. Energy (Oxford), 224, 120106. doi:10.1016/j.energy.2021.120106

Xylia, M., Leduc, S., Patrizio, P., Kraxner, F., & Silveira, S. (2017). Locating charging infrastructure for electric buses in Stockholm. Transportation Research. Part C, Emerging Technologies, 78(2017), 183-200. doi:10.1016/j.trc.2017.03.005

Yang, L., Yu, B., Yang, B., Chen, H., Malima, G., & Wei, Y.-M. (2021). Life cycle environmental assessment of electric and internal combustion engine vehicles in China. Journal of Cleaner Production, 285, 124899. doi:https://doi.org/10.1016/j.jclepro.2020.124899

Yu, R., Cong, L., Hui, Y., Zhao, D., & Yu, B. (2022). Life cycle CO2 emissions for the new energy vehicles in China drawing on the reshaped survival pattern. Science of the Total Environment, 826, 154102. doi:https://doi.org/10.1016/j.scitotenv.2022.154102

Zhang, X., Rey, D., & Waller, S. T. (2018). Multitype recharge facility location for electric vehicles. Computer-Aided Civil and Infrastructure Engineering, 33(11), 943-965. doi:10.1111/mice.12379

Zhou, Y., Wang, H., Wang, Y., & Li, R. (2022). Robust optimization for integrated planning of electric-bus charger deployment and charging scheduling. Transportation Research. Part D, Transport and Environment, 110. doi:10.1016/j.trd.2022.103410

Zhuge, C., & Shao, C. (2018). Agent-based modelling of locating public transport facilities for conventional and electric vehicles. Networks and Spatial Economics, 18(4), 875-908. doi:10.1007/s11067-018-9412-3